

Toward Nonaqueous Alkanolamine-Based Carbon Capture Systems: Developing Parameters for Systems Containing Glymes and Ethylene Glycols in s-SAFT- γ Mie

Alexander Schulze-Hulbe, Andries J. Burger, and Jamie T. Cripwell*



Cite This: *Ind. Eng. Chem. Res.* 2024, 63, 5912–5930



Read Online

ACCESS |

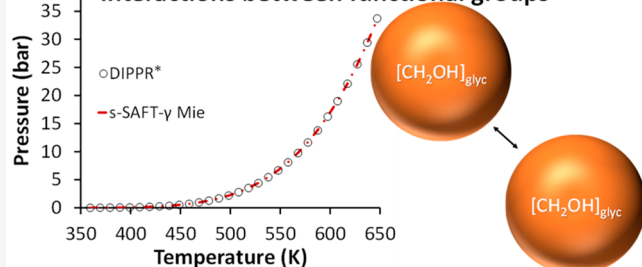
 Metrics & More

 Article Recommendations

 Supporting Information

ABSTRACT: High energy requirements are a key barrier to the wide-scale adoption of alkanolamine-based carbon capture processes. A potential solution to this issue may lie in replacing water, the traditional cosolvent, with an organic alternative. Accordingly, this work presents the continued parametrization of the s-SAFT- γ Mie predictive group-contribution equation of state toward a description of alkanolamine/CO₂/organic cosolvent systems. A consistent and systematic methodology is employed in extending s-SAFT- γ Mie to glymes and ethylene glycols and their mixtures with alkanolamines. s-SAFT- γ Mie provides robust qualitative descriptions of ethylene glycols and glymes as well as mono- and diethers. While model predictions are not always quantitative, the ability to obtain qualitatively meaningful results for a wide range of components with a single transferable parameter set underlines s-SAFT- γ Mie's broad applicability. This highlights s-SAFT- γ Mie's value in preliminary process design, where rapidly obtainable qualitative property estimates may be preferable to time- and resource-intensive measurements.

s-SAFT- γ Mie: predictive EoS that describes systems as interactions between functional groups



*Wilding et al., DIPPR Data Compilation of Pure Chemical Properties, Design Institute for Physical Properties, AIChE: New York, NY, 2022.

Downloaded via 144.48.80.102 on October 15, 2024 at 09:29:41 (UTC).
See https://pubs.acs.org/sharingguidelines for options on how to legitimately share published articles.

aqueous (organic) ones: organic cosolvents have lower heat capacities than water, and their heats of vaporization are lower.^{8,11} Indeed, computational studies by Bahamon et al.¹² and Alkhateeb et al.¹³ showed reduced energy consumption in nonaqueous alkanolamine-based carbon capture fluids. Moreover, Wanderley et al.¹⁴ concluded that nonaqueous cosolvents can certainly reduce the energy duties of alkanolamine-based carbon capture processes.

Additionally, nonaqueous alkanolamines promise lower temperatures for solvent regeneration,⁸ which may reduce solvent decomposition,^{15–19} evaporation,^{15–18} and corrosion,^{15–17,19} which are all major challenges in their own right.

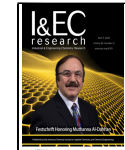
Yet there are also disadvantages to the use of nonaqueous alkanolamine formulations in carbon capture processes. For one, poorer heat transfer may require more expensive heat exchangers.¹⁴ The chief concern, however, is that CO₂ removal may be less efficient in nonaqueous process fluids,^{12,13,20,21} though this may not always be the case.

Received: January 8, 2024

Revised: March 5, 2024

Accepted: March 8, 2024

Published: March 25, 2024



1. INTRODUCTION

1.1. Nonaqueous Chemical Absorption Carbon Capture. Carbon capture and storage (CCS) technologies present a promising pathway to achieving meaningful reductions in CO₂ emissions in the near term.¹ Therefore, CCS technologies play a key role in the development of sustainable chemical and industrial processes. CCS can be applied in a diverse range of environments which include the cement sector,² the petrochemical and refining industries,³ biogas purification,⁴ and fossil-fuel-fired power plants.⁵

A common CCS approach is to remove CO₂ from industrial waste gases generated by the combustion of fossil fuels. This is commonly done by chemical absorption of CO₂ from these effluent gases into an aqueous solution of alkanolamines. The alkanolamines react with CO₂, thereby removing it from the waste gases. In-depth discussions of chemical absorption technology, and CCS more broadly, can be found in the works of Bui et al.³ and Mac Dowell et al.,¹ while a comprehensive review of chemical absorption-based CCS technology is provided by Liang et al.⁶

While alkanolamine-based chemical absorption is a mature technology, high energy requirements remain a key hurdle^{5,7–9} that must be overcome in order to render chemical absorption-based CCS technologies feasible for wide-scale use.¹⁰ One potential route for reducing these energy requirements is to replace the aqueous alkanolamine formulations with non-

It becomes evident that a holistic consideration of the effects of moving from aqueous to nonaqueous alkanolamines becomes important. A fundamental cornerstone of such a comparison is reliable thermodynamic modeling of both aqueous and nonaqueous alkanolamine-based carbon capture fluids. Indeed, phase equilibria are important for estimating energy requirements of carbon capture processes.²² Accordingly, this work specifically concerns itself with the thermodynamic modeling of glymes and ethylene glycols, which are important components of nonaqueous alkanolamine-based carbon capture systems.

1.2. SAFT Equations of State and the Group-Contribution Approach. A powerful approach to the thermodynamic modeling of carbon capture systems is posed by the Statistical Associating Fluid Theory (SAFT) equations of state (EoSs). These EoSs are fundamental modeling approaches, as they are rooted in the statistical mechanics framework of Wertheim's thermodynamic perturbation theory.^{23–26} In SAFT EoSs, molecules are composed of spherical segments arranged in a linear chain. Thermodynamic properties are determined from the Helmholtz free energies arising from the different types of interactions occurring between these segments. The addition of these free energies yields the residual Helmholtz free energy (A^{res}). This summation forms the mathematical backbone of SAFT and is shown in Equation 1.

$$A^{\text{res}} = A^{\text{hard sphere}} + A^{\text{dispersion}} + A^{\text{chain}} + A^{\text{association}} \quad (1)$$

$A^{\text{hard sphere}}$ and $A^{\text{dispersion}}$ arise from the hard sphere repulsive and dispersive interactions between segments, respectively. The Helmholtz free energy arising from the bonding of these segments to form chain-like molecules is given by A^{chain} . Finally, $A^{\text{association}}$ refers to the Helmholtz free energy contribution of highly directional association interactions between molecules (e.g., hydrogen bonding).

Equation 1 is a very versatile formulation: existing terms in the summation can be modified and improved, while additional terms can be added to account for a wide range of intermolecular interactions. This ensures that SAFT EoSs are highly flexible, thus enabling their application to a diverse range of challenging thermodynamic systems. These include hydrogen bonding fluids,^{27–31} polymers,^{32–39} and electrolytes.^{40–47} Further information regarding SAFT EoSs can be found in chapter 8 of ref 48 as well as in the reviews of Müller and Gubbins⁴⁹ and Tan et al.⁵⁰

SAFT EoSs have also been employed to model thermodynamic systems broadly relevant to CCS^{51–53} (e.g., flue gases and geological reservoir fluids). Moreover, extensive work has been done on modeling aqueous alkanolamine-based carbon capture systems with SAFT EoSs.^{54–65}

1.3. Predictive Modeling Approaches in the SAFT Context. A key advantage of using SAFT EoSs to model alkanolamine-based carbon capture systems lies in the development of predictive thermodynamic modeling approaches. These are particularly valuable for systems for which little or no data are available, as is the case for many nonaqueous alkanolamine-based carbon capture systems. One method leverages the finding that combinations of model parameters vary linearly with the molecular weight of species within a homologous series.^{66–68}

Another popular method for predictive thermodynamic modeling is the group contribution (GC) approach. In EoSs that use this approach, thermodynamic systems are modeled as interactions between functional groups, as opposed to molecules. Should parameters for the interaction between a system's functional groups exist, a wide range of other systems

consisting of the same groups can be modeled predictively with the same parameters. For instance, functional group interaction parameters can be determined from data for the propylamine/ethane system. These parameters can subsequently be transferred without modification to any system which features the same functional groups, such as the ethylamine/*n*-propane system. This is illustrated in Figure 1.

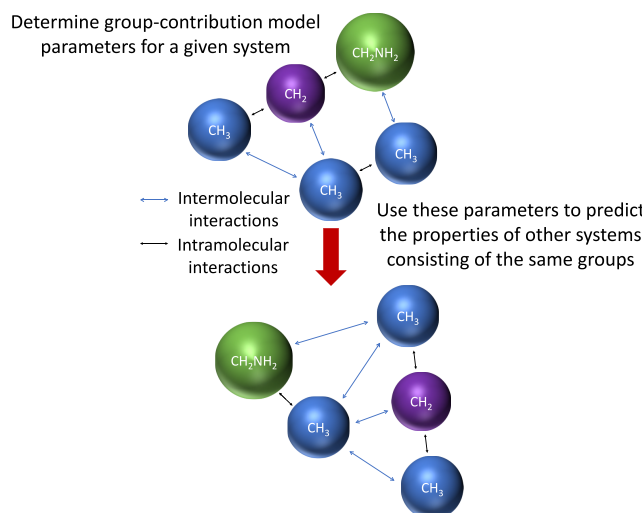


Figure 1. Illustration of how the group-contribution approach can be used for thermodynamic property prediction.

1.4. The Structural (s)-SAFT- γ Mie EoS. A particularly noteworthy GC-approach SAFT EoS is SAFT- γ Mie.⁶⁹ SAFT- γ Mie is the GC variant of the rigorous SAFT-VR Mie EoS,⁷⁰ which provides accurate descriptions of second-derivative properties and an improved description of the critical region.^{70–73} The combination of SAFT- γ Mie's rigorous physical foundation and the generalizability afforded by the GC approach has found successful application in a wide range of thermodynamic systems. These include electrolyte solutions,⁷⁴ pharmaceutical solutions,^{75,76} and aqueous alkanolamine systems.^{55,77} Haslam et al.⁷⁴ provide an overview of the diverse range of SAFT- γ Mie's applications.

Yet SAFT- γ Mie is unable to make distinctions between structural isomers. Consequently, Shaahmadi et al.⁷⁸ have modified SAFT- γ Mie to enable it to account for the subtle differences between isomers, resulting in the structural (s)-SAFT- γ Mie EoS. The accuracy of s-SAFT- γ Mie has been shown to rival that of SAFT- γ Mie for linear *n*-alkanes. It is further capable of accurately distinguishing between the isomers of branched species.⁷⁸ Subsequently, the model has been extended to primary alcohols.⁷⁹ s-SAFT- γ Mie's descriptions of primary alcohols and primary alcohol/*n*-alkane mixtures are comparable to those obtained with SAFT- γ Mie. Building on this work, Schulze-Hulbe et al.⁸⁰ subsequently extended s-SAFT- γ Mie toward a description of nonaqueous alkanolamine-based carbon capture systems. This entailed parametrizing the model for primary amines, secondary alcohols, and alkanolamines as well as CO₂-containing systems. Further discussion of the s-SAFT- γ Mie EoS and the combining rules employed can be found in previous work.^{78,79} As a state-of-the-art thermodynamic model, the s-SAFT- γ Mie EoS is well suited for use in describing alkanolamine/CO₂/organic cosolvent systems.

In the context of alkanolamine-based carbon capture, GC-approach EoSs such as s-SAFT- γ Mie are particularly useful.

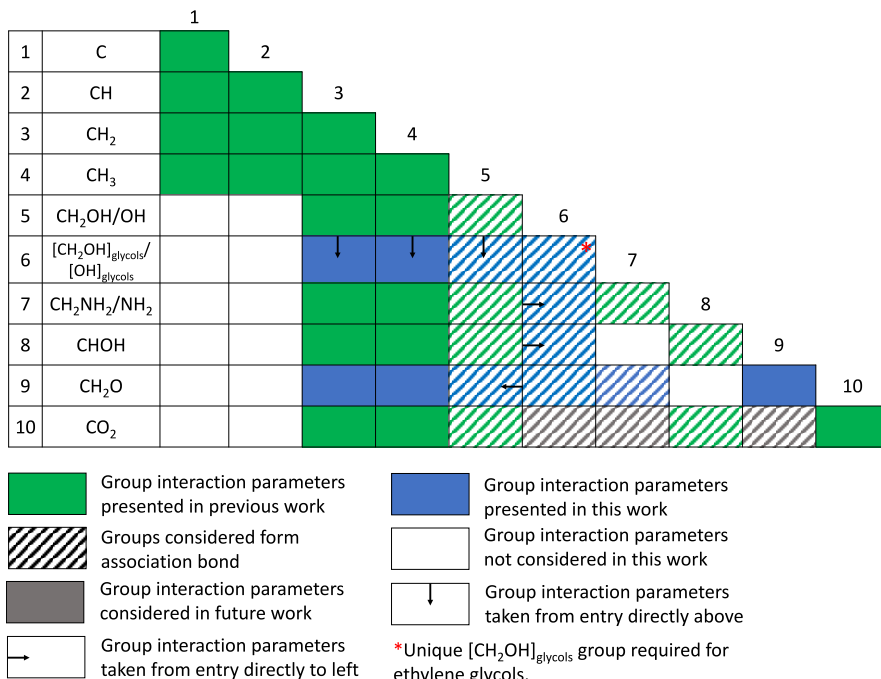


Figure 2. Current state of the s-SAFT- γ Mie group interaction parameter matrix.

Noting the broad range of possible alkanolamine solvent/cosolvent formulations, finding a suitable process fluid poses a formidable challenge. Accordingly, the predictive capabilities of GC-approach SAFT EoSs are very useful for screening novel solvent/cosolvent formulations, thereby guiding carbon capture process researchers and designers toward optimal process fluids. Indeed, the works of Papadopoulos et al.^{81,82} are illustrative examples of how GC-approach SAFT EoSs can be valuable tools for use within screening applications.

1.5. Aims and Objectives. Though SAFT- γ Mie has been applied to *aqueous* alkanolamine-based carbon capture systems,^{55,77} no GC-approach SAFT EoSs have been applied to modeling *nonaqueous* alkanolamine-based carbon capture systems to date. Despite their potential to reduce the high energy requirements of chemical absorption carbon capture, little attention has been paid to these nonaqueous alkanolamine/CO₂/organic cosolvent systems in the SAFT literature. The works of Alkhatib, Bahamon, and co-workers^{12,13,83,84} appear to be the only instances in which these ternary-component systems are treated within a traditional (non-group-contribution) SAFT framework.

Accordingly, this work presents the development of the s-SAFT- γ Mie group-contribution EoS toward modeling the thermodynamic properties of nonaqueous alkanolamine-based carbon capture systems. The aim of this work is to further parametrize s-SAFT- γ Mie toward ternary-component alkanolamine/CO₂/organic cosolvent systems.

s-SAFT- γ Mie's development for nonaqueous alkanolamine-based carbon capture requires a wide range of parameters, which are shown in the group interaction parameter matrix given in Figure 2.

Noting the large number of group interactions requiring parametrization, s-SAFT- γ Mie's development for nonaqueous alkanolamine-based carbon capture systems is presented in a series of publications. This work constitutes the second part in this series. Previously envisioned to be a two-part series,⁸⁰ a third publication will present the final model development of s-SAFT-

γ Mie for nonaqueous alkanolamine-based carbon capture systems.

Pertinently, this series of publications presents the first instance in which a group-contribution SAFT EoS is parametrized for nonaqueous alkanolamine-based carbon capture systems. This renders s-SAFT- γ Mie as the most broadly applicable predictive thermodynamic model developed toward these systems to date.

Significantly, there is a wide range of organic cosolvents that could be used in nonaqueous alkanolamine-based carbon capture. This work focuses on glymes and ethylene glycols, which have been investigated extensively as alternative cosolvents for several alkanolamines. Wanderley et al.¹⁴ and Heldebrant et al.⁸ refer to numerous investigations in which these chemical families have been investigated as water alternatives for alkanolamine-based carbon capture. In particular, the latter group highlights work done by Barzaghi and co-workers.^{15–17,21} Furthermore, the popular physical solvent Selexol⁸⁵ is a mixture of dialkyl glymes. This suggests that dialkyl glymes may make a noteworthy contribution to CO₂ solubility beyond alkanolamine-based chemical absorption, given their capabilities in absorbing CO₂ physically.

Ethylene glycols are defined as linear molecules that consist of repeating ethylene oxide ([OCH₂—CH₂—]_n) units and which terminate in hydroxyl (CH₂OH/OH) groups. Noting ambiguity regarding their definition in the literature, glymes are defined as follows in this work: linear molecules consisting of repeating ethylene oxide groups terminating *either* in one alkyl (CH₃—[CH₂—]_n) group and one hydroxyl group (monoalkyl glymes) or terminating only in alkyl groups (dialkyl glymes). Figure 3 illustrates these definitions with key glymes and ethylene glycols used in this work.

Seeing that the ether (CH₂O) functional group features prominently in glymes and ethylene glycols, a major aspect of this work is the development of the s-SAFT- γ Mie CH₂O group parameters. These are shown in row 9 in the parameter matrix given in Figure 2. The ether parameters are regressed from pure-

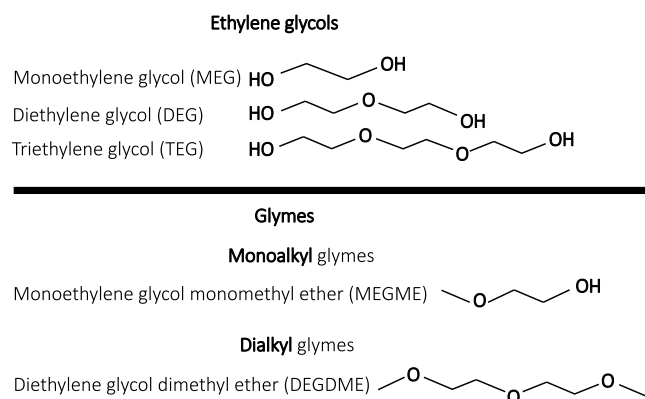


Figure 3. Illustration of ethylene glycols and glymes.

component glyme data as well as data for binary mixture subsystems (e.g., alkanolamine/glyme data). Using the ether parameters thus developed, s-SAFT- γ Mie is subsequently extended to ethylene glycols and alkanolamine/glyme mixtures.

In parametrizing GC SAFT EoSs such as s-SAFT- γ Mie, there is a very wide range of approaches that can be followed. As discussed previously,⁸⁰ the absence of a standardized approach to thermodynamic modeling is concerning for model users in industry⁸⁶ and poses a barrier to the use of advanced models in industrial settings. In light of this, a secondary aim of this work is to illustrate how group-contribution models can be parametrized consistently and systematically in the context of nonaqueous alkanolamine-based carbon capture fluids. The methodology used follows previous work on parametrizing s-SAFT- γ Mie for primary alcohols⁷⁹ and has also been implemented in previous work extending s-SAFT- γ Mie toward nonaqueous alkanolamine-based carbon capture systems.⁸⁰

Having provided an outline of this work, it is worth noting that the focus lies with modeling vapor–liquid equilibrium (VLE) data. This is justified by the fact that s-SAFT- γ Mie is developed for use in chemical absorption carbon capture applications,

which require reliable VLE descriptions. Nonetheless, the holistic design of chemical absorption carbon capture processes also requires caloric properties, such as the isobaric heat capacity and heat of vaporization. Moreover, the assessment of caloric properties is key in choosing suitable nonaqueous alkanolamine-based carbon capture formulations. Accordingly, a preliminary analysis of s-SAFT- γ Mie's capabilities in modeling these properties for glymes and ethylene glycols is provided at the end of this work.

2. METHODOLOGY

2.1. Parameter Fitting Procedure. The strategy employed in regressing s-SAFT- γ Mie parameters was discussed in previous work.⁸⁰ Further details regarding the data fitted to each set of group interaction parameters are given in Tables 1 and 2.

2.2. Thermodynamic Consistency Testing. Noting that mixture VLE data feature in s-SAFT- γ Mie's parametrization, the quality of the regressed mixture data is worth investigating. Such investigations are seldom performed in the SAFT literature. However, the extensive use of erroneous data in parameter fitting is ill-advised: it may yield parameter sets that are trained as much on measurement error as they are on the physics underlying the data, reducing a model's predictive capabilities.

An important set of methods for verifying the validity of phase equilibrium data are presented by thermodynamic consistency tests. These tests determine whether a set of VLE data conforms to the Gibbs–Duhem equation, the fundamental relation that underlies phase equilibria. It is worth noting that adherence to the Gibbs–Duhem equation is a necessary but not a sufficient criterion for accurate data. Should data obey the equation, they are consistent but may still be incorrect.⁹⁴ Yet consistency tests nonetheless present a fundamental method for assessing data quality. Accordingly, thermodynamic consistency testing is used as a criterion for accepting VLE data used in s-SAFT- γ Mie's development toward nonaqueous alkanolamine-based carbon capture.

Table 1. Fitting Procedure Details for Parameters Determined from Pure-Component Data^d

Functional group interactions parametrized	CH_2O with CH_2O , CH_3 and CH_2	$[\text{CH}_2\text{OH}]_{\text{glycols}} / [\text{OH}]_{\text{glycols}}$	$[\text{CH}_2\text{OH}]_{\text{glycols}} / [\text{OH}]_{\text{glycols}}$ with CH_2O
Parameter matrix references (Figure 2)	9–3, 9–4, 9–9	6–6	9–6
Species considered	Dialkyl glymes	Monoethylene glycol	Ethylene glycols
Functional groups present	CH_2O , CH_3 , CH_2	$[\text{CH}_2\text{OH}]_{\text{glycols}} / [\text{OH}]_{\text{glycols}}$, CH_3 , CH_2	$[\text{CH}_2\text{OH}]_{\text{glycols}} / [\text{OH}]_{\text{glycols}}$, CH_2O , CH_3 , CH_2
Site schemes considered	N/A (Non-self-associating species)	$[\text{CH}_2\text{OH}]_{\text{glycols}} / [\text{OH}]_{\text{glycols}}$: 2-site (1 e–1 H)	$[\text{CH}_2\text{OH}]_{\text{glycols}} / [\text{OH}]_{\text{glycols}}$: 2-site (1 e–1 H) CH_2O : 1-site (1 e) or 2-site (2 e)
Pure-component properties			
Species included	Diethylene glycol dimethyl ether to tetraethylene glycol dimethyl ether	Monoethylene glycol	Diethylene glycol to tetraethylene glycol
Regression weight for pure-component properties	1	1	1
Vapor pressure data: component used	Diethylene glycol dimethyl ether (25 points) ^a Triethylene glycol dimethyl ether (26 points) ^a Tetraethylene glycol dimethyl ether (25 points) ^a	Monoethylene glycol (30 points) ^c	Diethylene glycol (30 points) ^c Triethylene glycol (30 points) ^c
Saturated liquid density data: component used	Diethylene glycol dimethyl ether (25 points) ^a Triethylene glycol dimethyl ether (26 points) ^a Tetraethylene glycol dimethyl ether (30 points) ^b	Monoethylene glycol (30 points) ^c	Diethylene glycol (30 points) ^c Triethylene glycol (30 points) ^c Tetraethylene glycol (30 points) ^c

^aPseudoexperimental data taken from the NIST database.⁸⁷ ^bPseudoexperimental data taken from the DIPPR database (2020 version).⁸⁸

^cPseudoexperimental data taken from the DIPPR database (2022 version).⁸⁹ ^dAll pure-component data regressed between $0.5T_c$ and $0.9T_o$, where T_c is the critical temperature.

Table 2. Fitting Procedure Details for Parameters Determined from Binary Mixture Data

Functional group interactions parametrized	CH ₂ O with CH ₂ O, CH ₃ and CH ₂	CH ₂ O with CH ₂ NH ₂ /NH ₂
Parameter matrix references (Figure 2)	9–3, 9–4, 9–9	9–7
Species considered	Dialkyl glymes	Alkanolamines/mono- or dialkyl glymes
Functional groups present	CH ₂ O, CH ₃ , CH ₂	CH ₂ OH/OH, [CH ₂ OH] _{glycols} /[OH] _{glycols} , CH ₂ O, CH ₃ , CH ₂
Site schemes considered	N/A (Non-self-associating species)	CH ₂ OH/OH: 2-site (1 e–1 H) [CH ₂ OH] _{glycols} /[OH] _{glycols} : 2-site (1 e–1 H) CH ₂ O: 1-site (1 e) or 2-site (2 e)
Binary mixture data included	1,2-Diethoxyethane/ <i>n</i> -heptane ⁹⁰	a) Monoethanolamine/ monoethylene glycol monomethyl ether ⁹¹ b) Monoethanolamine/ diethylene glycol dimethyl ether ⁹² c) Butylamine/diethyl ether ⁹³ a) and b) Isobaric subcooled liquid density c) Excess enthalpy 1 a) 13 (293.15 K–353.15 K, 30 wt % Monoethanolamine) 13 (293.15 K–353.15 K, 70 wt % Monoethanolamine) b) 5 (293.15 K–333.15 K, 15 wt % Monoethanolamine) 5 (293.15 K–333.15 K, 30 wt % Monoethanolamine) 5 (293.15 K–333.15 K, 45 wt % Monoethanolamine) c) 12 (298.15 K)
Binary mixture data type	Isothermal VLE (343.13 K)	
Regression weight	1	
Number of data points	13	

A review of the consistency testing methods used in this work is presented in Section 1.2 of the *Supporting Information*. Following this, the consistency testing results for the data considered for use in this work as well as previous work⁸⁰ are presented in Section 1.3 of *Supporting Information*. Regarding phase equilibria data for CO₂-containing systems, only data sets for which a large majority of points are judged to be consistent are used in the model parametrization.

2.3. Determining Functional Groups and Choosing Association Sites. The ether group features prominently in the ethylene glycols and glymes treated in this work. Its structure is illustrated in Figure 4.

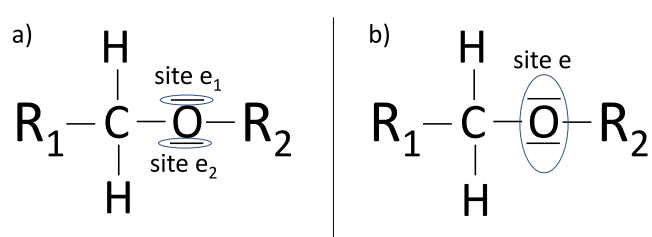


Figure 4. Illustration of the 2-site association scheme (a) and 1-site association scheme (b) for the ether group.

There are several ways in which ether-group-containing components can be split into functional groups. In the SAFT- γ Mie context, Burger et al.⁹⁵ modeled polyethers with fine-grained ether groups comprising a single oxygen atom as well as CH₂ and CH₃ groups. In this approach, the polarization of the electronegative oxygen atom on adjacent CH₂ and CH₃ groups is arguably accounted for implicitly in the energetic model parameters. Building on the work of Burger et al.,⁹⁵ Valsecchi et al.⁹⁶ subsequently introduced a unique CH₂ group for ethylene glycols to incorporate polarization effects by the oxygen atom.

Wu and Sandler suggest that a group's geometry and net charge should not depend on the molecule of which it is a part.⁹⁷ Accordingly, groups should be large enough so that polarization effects are encapsulated within the group, yielding a more electrically neutral coarse-grained group. This principle has guided the development of s-SAFT- γ Mie in previous work,^{79,80} culminating in the groups illustrated in Figure 2. Previously, exceptions have been made for the primary amine and primary alcohol groups. These are modeled with both coarse-(CH₂NH₂/CH₂OH) and fine-grained (NH₂/OH) groups.⁸⁰ The rationale for doing so is that these smaller groups are more versatile, which may provide benefits when the model is extended to branched species.

Considering this, a CH₂O group is chosen to model glymes and ethylene glycols with s-SAFT- γ Mie. This coarse-grained group presents a balance: while it accounts for the polarization effects of the oxygen on one of its adjacent CH₂ groups, its relatively small size enables its flexible use in a wide range of ether-containing components.

A unique terminal ether (CH₃O) group was also considered but ultimately not chosen: use of both a CH₂O and a CH₃O group resulted in poor predictions, suggesting that the large number of parameters afforded by using two distinct ether groups leads to overfitting.

Furthermore, Figure 4 shows that the ether group has two free electron pairs. Therefore, the formation of association bonds with other groups should be considered. In their review of SAFT modeling of CH₂O-group-containing species, Crespo and Coutinho⁹⁸ recognize that such bonds can form in ethylene glycols, which contain both CH₂O and CH₂OH/OH groups. However, these authors found that the associative CH₂O–CH₂OH/OH interactions are generally not considered in modeling ethylene glycols,⁹⁸ with the work of Breil and Kontogeorgis,⁹⁹ Qvistgaard et al.,¹⁰⁰ and Valsecchi et al.⁹⁶ being exceptions to this.

Considering the above, the presence of either 1 or 2 electron acceptor ("e") sites on the ether group will be considered. Both the 1 and 2 e-site schemes are shown in Figure 4. While these sites will be inactive when only ether and nonassociating groups are present, they will interact with any electron acceptor ("H") sites present in the system. More generally, considering all electron pairs as possible electron donor sites is also in line with the methodology employed in s-SAFT- γ Mie.

3. RESULTS AND DISCUSSION

3.1. Dialkyl Glymes. **3.1.1. Physical Significance of Ether Group (CH₂O) Parameters.** s-SAFT- γ Mie size and shape parameters are listed in Table 3. Table 4 provides the dispersion energies as well as the repulsive and attractive Mie exponents, whereas Table 5 shows the association parameters.

Table 4 shows that the dispersion energies for the CH₂O/CH₂O and CH₂O/CH₂ (CH₃) interactions lie in the range of ca. 270–350 K. This roughly agrees with the corresponding ranges

Table 3. s-SAFT- γ Mie Size and Shape Parameters

Group k	v_k^*	S_k	$\sigma_{kk}/\text{\AA}$	Group size ($v_k^* S_k \sigma_{kk}$)/ \AA
CH ₂ O	2	0.418	3.332	2.787
[CH ₂ OH] _{glycols} ^a	2	0.312	4.220	2.631
[OH] _{glycols} ^b	1	0.299	4.173	1.246

^aParameters taken from Schulze-Hulbe et al.⁷⁹ ^bParameters taken from Schulze-Hulbe et al.⁸⁰

for the CH₂OH group (320–400 K) and the CH₂NH₂ group (350–460 K). Table 3 provides the size of the CH₂O group. At 2.79 Å, it is larger than the CH₃ (2.03 Å) and CH₂ (1.36 Å) groups⁷⁸ and comparable in size to the CH₂OH group (2.63 Å).⁷⁹ Given the structural similarity between the CH₂O and CH₂OH groups, this is expected. The broad agreement between the CH₂O group parameters and those of other groups suggests that these parameters are physically meaningful.

3.1.2. Dialkyl Glyme Vapor Pressure and Saturated Liquid Density. For some dialkyl glymes, the arrangement of groups within a given component may have multiple permutations. For instance, diethylene glycol dibutyl ether can be modeled with two adjacent CH₂O groups or with CH₂ groups placed between CH₂O groups. These different arrangements are shown in Figure 5 below.

The arrangement chosen affects the s-SAFT- γ Mie chain term (A^{chain} in eq 1), leading to slightly different modeling results. To avoid ambiguity, the s-SAFT- γ Mie *a priori* parameters $v_{kl,i}$ and $v_{k,i}$ for the ethers considered in this work are given in Table S1 in the Supporting Information. Moreover, the $v_{kl,i}$ and $v_{k,i}$ parameters for ethylene glycols and monoalkyl glymes are given in Tables S2 to S5.

Table 6 shows s-SAFT- γ Mie vapor pressure and saturated liquid density descriptions of dialkyl glymes in terms of the percentage average absolute deviation (%AAD).

%AAD quantifies a model's ability to reproduce experimental data. This is defined in eq 2.

$$\%AAD = \frac{100}{n_M} \sum_{i=1}^{n_M} \left| \frac{M_i^{exp} - M_i^{calc}}{M_i^{exp}} \right| \quad (2)$$

Additionally, the model descriptions of dialkyl glyme vapor pressure and saturated liquid density are shown in Figure 6 (a) and (b), respectively.

Table 4. s-SAFT- γ Mie Dispersion Energies as Well as Repulsive and Attractive Mie Exponents

Group k	Group l	$(\epsilon_{kl}/k_B)/\text{K}$	λ_{kl}^r	λ_{kl}^a
Non-self-associating				
CH ₂ O	CH ₂ O	268.285	10.569	6.000
	CH ₃	340.747	CR ^a	CR ^a
	CH ₂	244.325	CR	CR
2-site [CH ₂ OH] _{glycols}	2-site [CH ₂ OH] _{glycols}	373.693	10.258	CR
2-site [OH] _{glycols}	2-site [OH] _{glycols}	513.209	8.605	CR
2-site [CH ₂ OH] _{glycols}	No sites CH ₂ O (no cross-association)	342.368	CR	CR
	1 e CH ₂ O	313.118	CR	CR
	2 e CH ₂ O	220.754	CR	CR
2-site [OH] _{glycols}	No sites CH ₂ O (no cross-association)	442.448	CR	CR
	1 e CH ₂ O	393.134	CR	CR
	2 e CH ₂ O	198.164	CR	CR
3-site CH ₂ NH ₂	1 e CH ₂ O	416.565	CR	CR
3-site NH ₂	1 e CH ₂ O	491.683	CR	CR

^aCR: Combining rule for repulsive (λ_{kl}^r) and attractive (λ_{kl}^a) exponents given by Haslam et al.⁷⁴

Pure-component data were drawn from both the NIST⁸⁷ and DIPPR^{88,89} databases. If a component was available in both databases, then the one with the lowest estimated error was chosen. Furthermore, the data were deemed acceptable for regression only if the estimated error was suitably low (below ca. 5%).

Figure 6 (a) shows that s-SAFT- γ Mie provides qualitatively meaningful descriptions of dialkyl glyme vapor pressures. Table 6 provides an average %AAD of 7.0% for fitted vapor pressures and 10.4% for predictions. Quantitatively accurate descriptions are not expected: Crespo and Coutinho¹⁰¹ found that SAFT- γ Mie provides poor phase equilibria descriptions of the series of dimethyl glymes from diethylene glycol dimethyl ether to tetraethylene glycol dimethyl ether, with an average vapor pressure %AAD of ca. 39%. Yet these modeling results are not directly comparable, given that these authors transferred parameters from monoalkyl glymes to dialkyl glymes and included a unique dialkyl glyme end group (OCH₃).

Furthermore, Figure 6 (b) shows that s-SAFT- γ Mie provides robust descriptions of the saturated liquid density, with an average %AAD of 1.8% for correlated data and 2.0% for predictions.

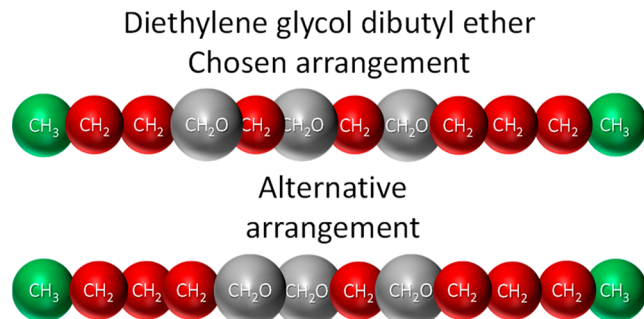
Given their promise as useful carbon capture fluids, s-SAFT- γ Mie specifically targets long-chained ethers such as dialkyl glymes. However, to assess the model's capabilities, predictions of short-chained ether phase behavior are also investigated. Table 7 provides %AAD values of s-SAFT- γ Mie predictions of mono- and diether vapor pressures and saturated liquid density. The corresponding model predictions of mono- and diether phase behavior are also shown in Figures 7 and 8, respectively.

Figures 7 and 8 show that s-SAFT- γ Mie qualitatively captures the effect of changes in chain length on mono- and diether vapor pressure and saturated liquid density. However, Table 7 indicates that model performance for mono- and diethers does not extend to quantitative accuracy: the average vapor pressure %AAD is 10.0% for monoethers, though %AAD values vary between 4.0% and 18.7%. For diethers, the variation in vapor pressure %AAD is again significant (7.1 to 48.0%), with an average %AAD of 20.2%.

However, accurate model predictions are not expected: Burger et al.⁹⁵ found that SAFT- γ Mie provides vapor pressure %AADs ranging from ca. 4 to 25% for mono- and diethers.

Table 5. s-SAFT- γ Mie Association Parameters

Group <i>k</i>	Group <i>l</i>	Site type <i>a</i> on group <i>k</i> (no. of occurrences)	Site type <i>b</i> on group <i>l</i> (no. of occurrences)	$(\varepsilon_{kl,ab}^{HB}/k_B)/K$	$k_{kl,ab}^{HB}/\text{Å}^3$
2-site [CH ₂ OH] _{glycols}	2-site [CH ₂ OH] _{glycols}	H (1)	e (1)	2511.614	43.635
2-site [OH] _{glycols}	2-site [OH] _{glycols}	H (1)	e (1)	2497.384	42.641
2-site [CH ₂ OH] _{glycols}	1 e CH ₂ O	H (1)	e (1)	406.448	1327.464
	2 e CH ₂ O	H (1)	e (2)	1654.535	191.719
2-site [OH] _{glycols}	1 e CH ₂ O	H (1)	e (1)	439.376	1017.411
	2 e CH ₂ O	H (1)	e (2)	1687.023	189.216
3-site CH ₂ NH ₂	1 e CH ₂ O	H (2)	e (1)	417.258	325.975
3-site NH ₂	1 e CH ₂ O	H (2)	e (1)	669.360	142.009

**Figure 5.** Illustration of different structural arrangements for diethylene glycol dibutyl ether in s-SAFT- γ Mie.

To date, s-SAFT- γ Mie has performed well in parametrizing families in which the functional group of interest occurs only once per molecule (e.g., primary and secondary alcohols, primary amines). It is possible that the complexities introduced by multiple occurrences of the target functional group (CH₂O) on a single component are more challenging to reproduce or that modeling these groups as “multiple occurrences” is too simplistic. This may in part account for the model’s lack of quantitative accuracy for ethers.

Supporting this notion is the fact that the model exhibits, on average, significantly poorer vapor pressure predictions for diethers (two CH₂O groups, 20.2% average %AAD) than for monoethers (one CH₂O group, 10.0% average %AAD). However, in comparing %AAD values of mono- and diethers, it should be borne in mind that diethers tend to have lower vapor pressures than monoethers. This results in a smaller denominator in eq 2, which may, in turn, yield higher %AAD values for diethers relative to those for monoethers. This indicates that rigorous comparison of the results for mono- and

diethers can be challenging when the %AAD metric is used. Nonetheless, further evidence for the improved results for monoethers over diethers can be found in Figures 7 and 8, which show that the s-SAFT- γ Mie vapor pressure predictions for monoethers are generally much improved relative to those for diethers.

In light of the robust qualitative descriptions of dialkyl glymes as well as mono- and diethers, the s-SAFT- γ Mie CH₂O group parameters thus discussed are further transferred to ethylene glycols. This is in line with the inherently predictive approach taken in parametrizing s-SAFT- γ Mie.

3.2. Developing Unique Ethylene Glycol Hydroxyl Group Parameters. A key aspect of GC-approach thermodynamic modeling of ethylene glycols is providing an accurate representation of the terminal hydroxyl group. However, the existing primary alcohol parameters provide inadequate predictions of the vapor pressure of the shortest of the ethylene glycols, viz., monoethylene glycol. This is illustrated in Figure 9, which shows the vapor pressure and saturated liquid density data for monoethylene glycol. The dashed black and blue lines show the predictions obtained with the OH and CH₂OH groups, respectively. The former has a vapor pressure %AAD value of 48.1%, whereas the latter has a %AAD value of 48.9%.

However, poor performance is arguably to be expected when using parameters regressed on *monoalcohols* (which feature a single hydroxyl group) for *dialcohols* (which possess two terminal hydroxyl groups). Figure 10 shows VLE data for the monoethylene glycol/ethanol mixture.¹⁰²

Figure 10 shows that the pure-component boiling points differ by 120 K between the shortest monoalcohol that features the CH₂OH group (ethanol) and the analogous dialcohol (monoethylene glycol). This suggests that mono- and dialcohols differ fundamentally in terms of fluid structure as well as inter- and

Table 6. %AAD of Saturated Vapor Pressure (P^{sat}) and Saturated Liquid Density (ρ_{liq}^{sat}) Descriptions of Dialkyl Glymes Obtained with s-SAFT- γ Mie

	Acronym	Temperature range (K)	N_{pts}	Data source	P^{sat} %AAD	Temperature range (K)	N_{pts}	Data source	ρ_{liq}^{sat} %AAD
Correlated data for dimethyl glymes: CH ₃ -[OCH ₂ -CH ₂] _{<i>n</i>} -O-CH ₃									
Diethylene glycol dimethyl ether	DEGDME	310–555	25	NIST ⁸⁷	4.97	310–555	25	NIST ⁸⁷	1.65
Triethylene glycol dimethyl ether	TEGDME	330–596	26	NIST ⁸⁷	9.68	330–593	26	NIST ⁸⁷	2.23
Tetraethylene glycol dimethyl ether	TetEGDME	359–642	25	NIST ⁸⁷	6.38	353–635	30	DIPPR ⁸⁸	1.53
Average					7.01				1.80
Predicted data for dialkyl glymes: CH ₃ -[CH ₂] _{<i>n</i>₁} -[OCH ₂ -CH ₂] _{<i>n</i>₂} -O-[CH ₂] _{<i>n</i>₃} -CH ₃									
Diethylene glycol diethyl ether	DEGDEE	317–571	30	NIST ⁸⁷	12.11	310–555	25	NIST ⁸⁷	2.64
Diethylene glycol dipropyl ether	DEGDPE	330–587	24	NIST ⁸⁷	8.56	330–593	26	NIST ⁸⁷	1.51
Diethylene glycol dibutyl ether	DEGDBE	340–612	30	DIPPR ⁸⁹	10.64	353–635	30	DIPPR ⁸⁹	1.98
Average					10.44				2.04

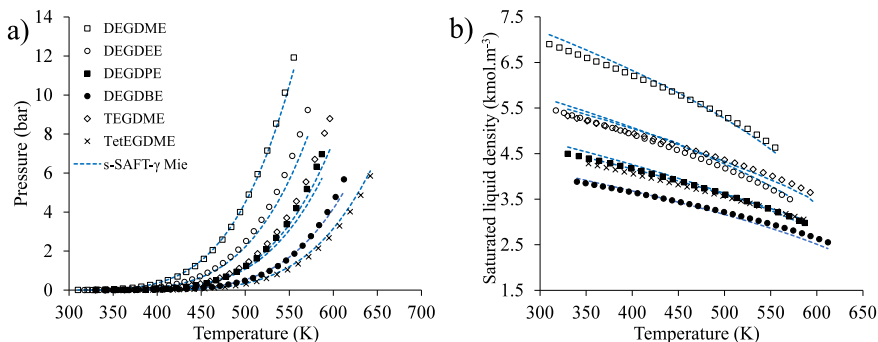


Figure 6. Saturated vapor pressures (a) and saturated liquid densities (b) for dialkyl glymes obtained with an s-SAFT- γ Mie. Acronyms in the legend are explained in Table 6. Table 6 further indicates whether pseudoexperimental data for a given component were obtained from the DIPPR^{88,89} or NIST⁸⁷ databases.

Table 7. %AAD of Saturated Vapor Pressure (P^{sat}) and Saturated Liquid Density (ρ_{liq}^{sat}) Predictions of Mono- and Diethers Obtained with s-SAFT- γ Mie

	Temperature range (K)	N_{pts}	Data source	P^{sat} %AAD	ρ_{liq}^{sat} %AAD
Predictions: Monoethers ($\text{CH}_3-\text{[CH}_2]_{n_1}-\text{OCH}_2-\text{[CH}_2]_{n_2}-\text{CH}_3$)					
Diethyl ether	233–420	30	DIPPR ⁸⁹	18.66	4.66
Dipropyl ether	265–478	30	DIPPR ⁸⁹	15.82	2.12
Dibutyl ether	292–526	30	DIPPR ⁸⁹	7.44	1.11
Dipentyl ether	311–560	30	DIPPR ⁸⁹	5.17	1.00
Dihexyl ether	392–592	30	DIPPR ⁸⁹	13.22	1.57
Methyl ethyl ether	219–394	30	DIPPR ⁸⁹	3.46	2.23
Methyl propyl ether	238–429	30	DIPPR ⁸⁹	4.04	2.80
Methyl butyl ether	256–462	30	DIPPR ⁸⁹	7.31	1.09
Methyl pentyl ether	273–492	30	DIPPR ⁸⁹	15.93	0.96
Ethyl propyl ether	250–450	30	DIPPR ⁸⁹	10.55	4.32
Ethyl hexyl ether	292–525	30	DIPPR ⁸⁹	8.00	0.95
Average				9.96	2.07
Predictions: Diethers ($\text{CH}_3-\text{[CH}_2]_{n_1}-\text{OCH}_2-\text{[CH}_2]_{n_2}-\text{OCH}_2-\text{[CH}_2]_{n_3}-\text{CH}_3$)					
1,4-Dipropoxybutane	319–577	25	NIST ⁸⁷	11.64	1.67
1,1-Dipropoxymethane	267–478	27	NIST ⁸⁷	48.03	6.71
1-Methoxy-1-butoxymethane	279–504	24	NIST ⁸⁷	18.95	3.23
1,2-Dibutoxyethane	314–569	24	NIST ⁸⁷	9.96	1.05
1-Ethoxy-2-propoxyethane	286–510	24	NIST ⁸⁷	33.82	3.57
1,2-Dipropoxyethane	302–538	24	NIST ⁸⁷	13.95	1.47
1,2-Dimethoxyethane	268–483	30	DIPPR ⁸⁸	7.12	2.62
1,2-Diethoxyethane	283–509	30	DIPPR ⁸⁸	18.00	2.81
Average				20.18	2.89

intramolecular interaction. This arguably justifies the modification of the existing primary alcohol parameters in extending s-SAFT- γ Mie to ethylene glycols, which are dialcohols. Moreover, differentiating between hydrogen bonding in ethylene glycols and other hydroxyl-group containing components is not without precedent in developing group-contribution models. In their soft-SAFT model for nonaqueous alkanolamine-based carbon capture, Alkhatab et al.¹³ used hydroxyl-hydroxyl association parameters for ethylene glycols distinct from the alkanolamine hydroxyl-hydroxyl parameters.

Modifying a functional group to account for its unique molecular environment is termed developing second-order groups. The original CH_2OH (OH) parameters previously

parametrized with primary alcohol (i.e., monoalcohol) data are modified to yield the $[\text{CH}_2\text{OH}]_{\text{glycols}}$ and $[\text{OH}]_{\text{glycols}}$ ethylene glycol second-order groups. These are developed by regressing the $\text{CH}_2\text{OH}-\text{CH}_2\text{OH}$ (OH–OH) dispersion energy (e_{kl}/k_B), association energy ($e_{kl,ab}^{\text{HB}}/k_B$), and association volume ($\kappa_{kl,ab}^{\text{HB}}$) to pure-component vapor pressure and saturated liquid density data for monoethylene glycol.

Modification of the $\text{CH}_2\text{OH}-\text{CH}_2\text{OH}$ (OH–OH) interaction is clearly needed, as evidenced by the poor results obtained for monoethylene glycol with the original parameters. However, in keeping with the predictive nature of the model, all other interactions are retained. This means that the $[\text{CH}_2\text{OH}]_{\text{glycols}}$ and $[\text{OH}]_{\text{glycols}}$ groups are completely identical to the CH_2OH and OH groups, except for the $[\text{CH}_2\text{OH}]_{\text{glycols}}-[\text{CH}_2\text{OH}]_{\text{glycols}}$ ($[\text{OH}]_{\text{glycols}}-[\text{OH}]_{\text{glycols}}$) interaction between hydroxyl groups on ethylene glycols. For instance, the $[\text{CH}_2\text{OH}]_{\text{glycols}}-\text{CH}_2\text{NH}_2$ and $[\text{CH}_2\text{OH}]_{\text{glycols}}-\text{CH}_2\text{OH}$ interaction parameters are the same as the corresponding $\text{CH}_2\text{OH}-\text{CH}_2\text{NH}_2$ and $\text{CH}_2\text{OH}-\text{CH}_2\text{OH}$ parameters, respectively. The reader is referred to Figure 2 for an overview of the $[\text{CH}_2\text{OH}]_{\text{glycols}}$ parameters. In the continued development of s-SAFT- γ Mie, instances in which the $[\text{CH}_2\text{OH}]_{\text{glycols}}$ ($[\text{OH}]_{\text{glycols}}$) parameters differ from those of the original CH_2OH (OH) groups are clearly indicated.

The $[\text{CH}_2\text{OH}]_{\text{glycols}}$ and $[\text{OH}]_{\text{glycols}}$ parameters are given in Tables 4 and 5. As previously found for the CH_2OH (OH) and CH_2NH_2 (NH_2) groups,⁸⁰ the dispersion energy of the fine-grained group is larger than that of the coarse-grained one. It was previously⁸⁰ postulated that this arises because the smaller group is more polar than the electrically neutral larger group. The polarity may well be accounted for by the dispersion term, thereby resulting in a larger dispersion energy.⁸⁰

Figure 9 illustrates that both groups provide accurate descriptions of vapor pressure (a %AAD value of 0.3% for both the $[\text{CH}_2\text{OH}]_{\text{glycols}}$ and $[\text{OH}]_{\text{glycols}}$ groups) and saturated liquid density (a %AAD value of 2.0% for both groups).

It is stressed that the $\text{CH}_2\text{OH}-[\text{CH}_2\text{OH}]_{\text{glycols}}$ ($\text{OH}-[\text{OH}]_{\text{glycols}}$) interaction is taken as the original $\text{CH}_2\text{OH}-\text{CH}_2\text{OH}$ (OH–OH) interaction. Such interactions between the original and ethylene glycol hydroxyl groups occur in alkanolamine/ethylene glycol or primary alcohol/ethylene glycol systems. Figure 10 shows predictions for the ethanol/monoethylene glycol VLE obtained with these transferred interaction parameters. Figure 1 shows that the prediction of the ethanol/monoethylene glycol system is qualitatively accurate. This suggests that these transferred $\text{CH}_2\text{OH}-[\text{CH}_2\text{OH}]_{\text{glycols}}$ ($\text{OH}-$

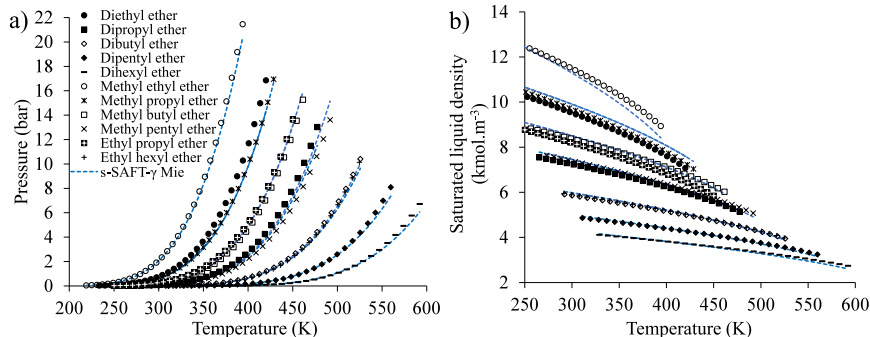


Figure 7. Saturated vapor pressures (a) and saturated liquid densities (b) for monoethers obtained with s-SAFT- γ Mie. Pseudoexperimental data were obtained from the DIPPR⁸⁹ database.

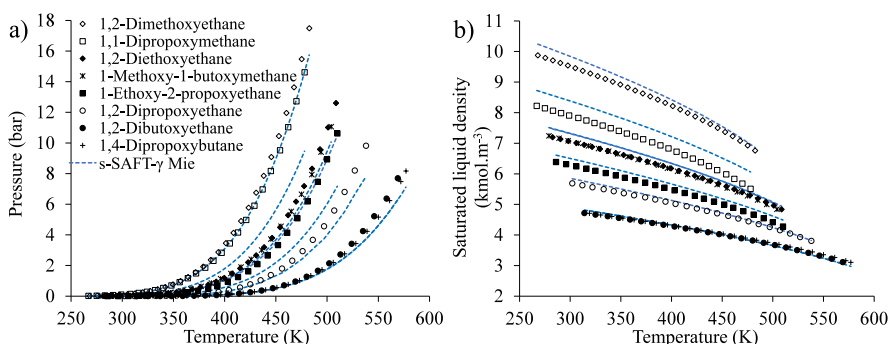


Figure 8. Saturated vapor pressures (a) and saturated liquid densities (b) for diethers obtained with s-SAFT- γ Mie. Table 7 indicates whether pseudoexperimental data for a given component were taken from the DIPPR^{88,89} or NIST⁸⁷ database.

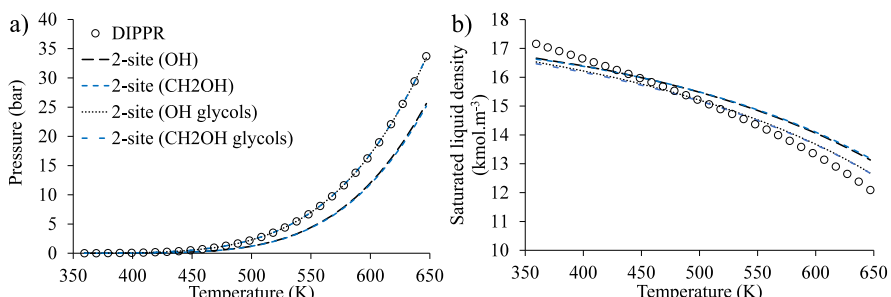


Figure 9. Monoethylene glycol saturated vapor pressure (a) and saturated liquid density (b) obtained with s-SAFT- γ Mie. “DIPPR” refers to pseudoexperimental data obtained from the DIPPR database.⁸⁹

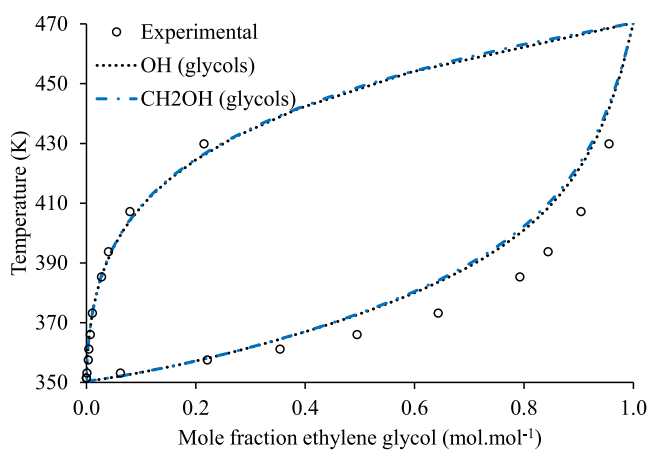


Figure 10. Isobaric binary VLE predictions for the monoethylene glycol/ethanol system at 1.013 bar. Experimental data taken from Li et al.¹⁰²

[OH]_{glycols}) parameters are suitable for use in the model's further development.

Consistent with the inherently predictive nature of the model, the [CH₂OH]_{glycols}–[CH₂OH]_{glycols} ([OH]_{glycols}–[OH]_{glycols}) interaction parameters are parametrized solely on monoethylene glycol and transferred to higher ethylene glycols without further modification.

3.3. Ethylene Glycols: Pure-Component Properties and Mixtures with *n*-Alkanes. Having developed CH₂O group parameters as well as [CH₂OH]_{glycols} ([OH]_{glycols}) parameters, these are transferred predictively to ethylene glycols.

Extending s-SAFT- γ Mie to ethylene glycols entails developing model parameters for the [CH₂OH]_{glycols} ([OH]_{glycols})–CH₂O interaction. As outlined in Section 2.3, a 1 e-site, a 2 e-site, and a no e-site scheme are all considered for the CH₂O group in modeling ethylene glycols.

Table 5 shows that the 2-site [CH₂OH]_{glycols} ([OH]_{glycols})–1 e-site CH₂O parameter sets exhibit particularly low association energies (ca. 400 K) and unusually high association volumes (ca.

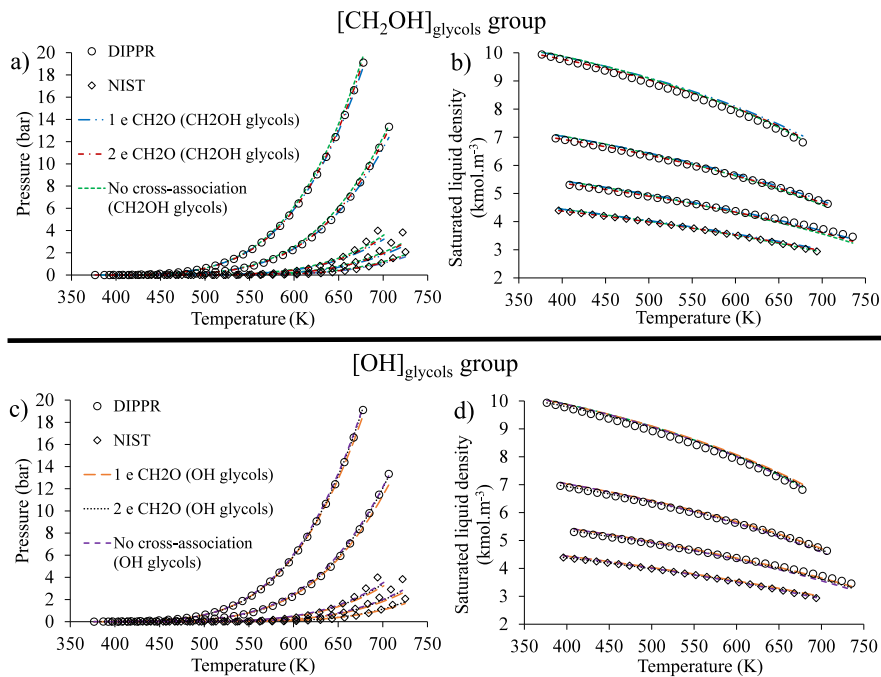


Figure 11. (a) and (c) Saturated vapor pressures for diethylene glycol to heptaethylene glycol obtained with s-SAFT- γ Mie using the $[\text{CH}_2\text{OH}]_{\text{glycols}}$ and $[\text{OH}]_{\text{glycols}}$ groups, respectively. Tetraethylene glycol is excluded, and the chain length increases from left to right. (b) and (d) Saturated liquid densities of diethylene glycol to pentaethylene glycol obtained with s-SAFT- γ Mie using the $[\text{CH}_2\text{OH}]_{\text{glycols}}$ and $[\text{OH}]_{\text{glycols}}$ groups, respectively. The chain length increases from top to bottom. “DIPPR” and “NIST” refer to pseudoexperimental data obtained from the DIPPR⁸⁹ and NIST⁸⁷ databases, respectively.

1000 Å³). This may indicate that the association energy and volume are strongly correlated, rendering a wide range of suitable combinations of these two parameters. As physically meaningful model parameters are desirable, the unusual values obtained for this parameter set should be borne in mind when deciding which parameter set to carry forward in the model’s development.

Figure 11 provides s-SAFT- γ Mie descriptions of ethylene glycol vapor pressure and saturated liquid density obtained with the $[\text{CH}_2\text{OH}]_{\text{glycols}}$ and $[\text{OH}]_{\text{glycols}}$ groups. The vapor pressure of tetraethylene glycol was omitted in this work, given the higher uncertainty of the data in both the DIPPR⁸⁹ and NIST databases.⁸⁷

Figure 11 shows that, for all schemes considered, the overall description of saturated liquid density was accurate, with average %AAD values ranging between 0.9 and 1.6% for all schemes considered. This holds true for both the $[\text{CH}_2\text{OH}]_{\text{glycols}}$ and $[\text{OH}]_{\text{glycols}}$ groups.

Furthermore, Figure 11 illustrates that s-SAFT- γ Mie provides an accurate correlation to diethylene and triethylene glycol vapor pressures when $[\text{CH}_2\text{OH}]_{\text{glycols}} - \text{CH}_2\text{O}$ cross-association is considered: The average %AAD values are 2.8% for the 1 e-site CH_2O scheme, whereas the 2 e-site scheme yielded values of 2.4% with the $[\text{CH}_2\text{OH}]_{\text{glycols}}$ group. Results obtained with the $[\text{OH}]_{\text{glycols}}$ group are very similar. However, neglecting cross-association yields a higher average %AAD value of 6.0% for the correlated vapor pressures with the $[\text{CH}_2\text{OH}]_{\text{glycols}}$ group (5.0% for the $[\text{OH}]_{\text{glycols}}$ group). This suggests that cross-association between the CH_2O and $[\text{CH}_2\text{OH}]_{\text{glycols}}$ ($[\text{OH}]_{\text{glycols}}$) groups should be incorporated into the model, echoing the conclusions of Crespo and Coutinho.¹⁰¹

Moreover, the vapor pressures of higher ethylene glycols (pentaethylene to heptaethylene glycol) are predicted with

qualitative as opposed to quantitative accuracy in all cases. In considering these predictions, it is important to note that s-SAFT- γ Mie’s parametrization is at an advanced stage. It is therefore worth discussing the trade-off between generalizability and predictive accuracy, which is inherent in the group-contribution approach. This trade-off becomes important as model development progresses.

Transfer of group interaction parameters between systems underpins s-SAFT- γ Mie’s predictive capabilities. However, a given group–group interaction does not truly remain fixed but will differ between systems. Therefore, transferring group interaction parameters to new systems without modification introduces numerous approximations that accumulate as the parameter matrix expands. Accordingly, new group interaction parameters developed for a given system must compensate for these approximations in addition to representing the group interaction of interest. Naturally, this affects the developed parameters’ predictive capabilities, rendering quantitatively accurate prediction progressively more challenging as s-SAFT- γ Mie is extended to increasingly complex systems. This may well account for the lack of quantitative accuracy for the higher ethylene glycols.

Moreover, it should be borne in mind that $[\text{CH}_2\text{OH}]_{\text{glycols}} - [\text{CH}_2\text{OH}]_{\text{glycols}}$ ($[\text{OH}]_{\text{glycols}} - [\text{OH}]_{\text{glycols}}$) association interactions are transferred from monoethylene glycol and that $[\text{CH}_2\text{OH}]_{\text{glycols}} - \text{CH}_2\text{O}$ ($[\text{OH}]_{\text{glycols}} - \text{CH}_2\text{O}$) interactions are taken from diethylene and triethylene glycol. Accordingly, parameters obtained from the shortest ethylene glycols are used to model longer-chained ones. It is possible that the considerable length of the higher ethylene glycols prevents hydrogen bonding between hydroxyl groups, thereby reducing the significance of association interactions for longer components. Brinkley and Gupta¹⁰³ have compared the extent of hydrogen bonding in two monoalkyl glymes (monoethylene

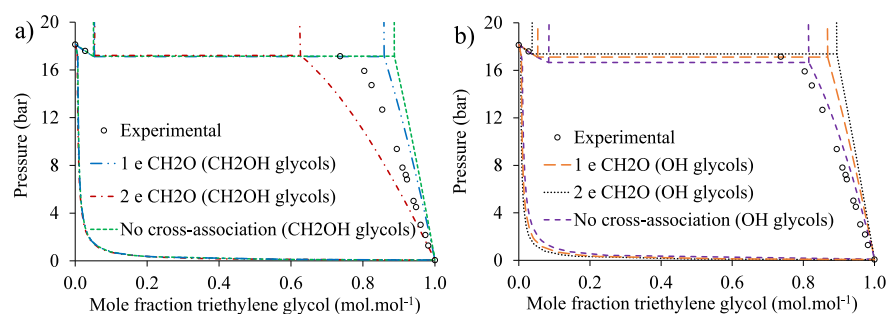


Figure 12. Isothermal binary VLE predictions for the triethylene glycol/*n*-hexane system at 473 K obtained with s-SAFT- γ Mie using the $[\text{CH}_2\text{OH}]_{\text{glycols}}$ group (a) and the $[\text{OH}]_{\text{glycols}}$ group (b). Experimental data are taken from Rowley et al.¹⁰⁴

Table 8. %AAD of Saturated Vapor Pressure (P^{sat}) Predictions of Monoalkyl Glymes Obtained with s-SAFT- γ Mie Using the $[\text{CH}_2\text{OH}]_{\text{glycols}}$ Group

Hydroxyl group	2-site $[\text{CH}_2\text{OH}]_{\text{glycols}}$			Ref		
	Ether group		$P^{\text{sat}} \text{ %AAD}$			
	Temperature range (K)	N_{pts}				
Monoethylene glycol monomethyl ether	302–537	46	11.13	8.00	2.88	NIST ⁸⁷
Monoethylene glycol monoethyl ether	303–539	46	16.57	14.00	21.67	NIST ⁸⁷
Monoethylene glycol monopropyl ether	307–552	47	20.77	19.76	29.91	NIST ⁸⁷
Monoethylene glycol monobutyl ether	320–569	47	13.33	13.31	25.79	NIST ⁸⁷
Diethylene glycol monomethyl ether	336–604	30	14.11	12.41	4.30	DIPPR ⁸⁹
Diethylene glycol monoethyl ether	335–603	30	6.30	3.30	10.35	DIPPR ⁸⁹
Diethylene glycol monopropyl ether	340–610	47	7.46	7.89	19.47	NIST ⁸⁷
Diethylene glycol monobutyl ether	346–623	30	8.33	4.97	12.91	DIPPR ⁸⁹
Triethylene glycol monomethyl ether	329–592	30	14.58	14.83	21.90	DIPPR ⁸⁹
Triethylene glycol monoethyl ether	337–606	30	23.22	24.31	15.00	DIPPR ⁸⁹
Triethylene glycol monopropyl ether	342–616	30	14.90	13.64	11.69	DIPPR ⁸⁹
Triethylene glycol monobutyl ether	356–629	30	14.47	17.38	21.65	NIST ⁸⁷
Tetraethylene glycol monomethyl ether	388–685	46	18.80	23.46	28.60	NIST ⁸⁷
Tetraethylene glycol monobutyl ether	376–674	47	8.32	10.61	21.00	NIST ⁸⁷
Average			13.73	13.42	17.65	

Table 9. %AAD of Saturated Liquid Density ($\rho_{\text{liq}}^{\text{sat}}$) Predictions of Monoalkyl Glymes Obtained with s-SAFT- γ Mie by Using the $[\text{CH}_2\text{OH}]_{\text{glycols}}$ Group

Hydroxyl group	2-site $[\text{CH}_2\text{OH}]_{\text{glycols}}$			Ref		
	Ether group		$\rho_{\text{liq}}^{\text{sat}} \text{ %AAD}$			
	Temperature range (K)	N_{pts}				
Monoethylene glycol monomethyl ether	302–537	46	1.16	1.22	0.64	NIST ⁸⁷
Monoethylene glycol monoethyl ether	285–512	30	2.11	2.21	1.80	DIPPR ⁸⁹
Monoethylene glycol monopropyl ether	307–552	47	2.58	2.88	3.17	NIST ⁸⁷
Monoethylene glycol monobutyl ether	317–571	30	1.18	1.54	2.20	DIPPR ⁸⁹
Diethylene glycol monomethyl ether	340–600	46	1.29	1.05	0.34	NIST ⁸⁷
Diethylene glycol monoethyl ether	339–603	47	1.41	1.59	1.18	NIST ⁸⁷
Diethylene glycol monopropyl ether	340–610	47	1.61	1.56	1.51	NIST ⁸⁷
Diethylene glycol monobutyl ether	346–623	30	1.92	1.42	1.01	DIPPR ⁸⁹
Triethylene glycol monomethyl ether	329–592	30	3.48	4.03	2.97	DIPPR ⁸⁹
Triethylene glycol monoethyl ether	372–693	51	4.76	3.71	3.82	NIST ⁸⁷
Triethylene glycol monopropyl ether	342–616	30	1.91	2.58	2.44	DIPPR ⁸⁹
Triethylene glycol monobutyl ether	348–626	30	0.63	1.10	1.24	DIPPR ⁸⁹
Tetraethylene glycol monomethyl ether	388–685	46	4.89	3.83	4.50	NIST ⁸⁷
Tetraethylene glycol monobutyl ether	376–674	47	3.05	2.28	2.09	NIST ⁸⁷
Average			2.28	2.21	2.06	

glycol monomethyl ether and monoethylene glycol monobutyl ether) using infrared spectroscopy. These authors found that the degree of hydrogen bonding decreases with chain length, which they attributed to steric hindrance.¹⁰³ It is therefore plausible

that higher ethylene glycols exhibit similar steric hindrance effects, which are not accounted for by s-SAFT- γ Mie.

In the broader practical context of the study, the increased viscosities of longer-chained ethylene glycols may render them

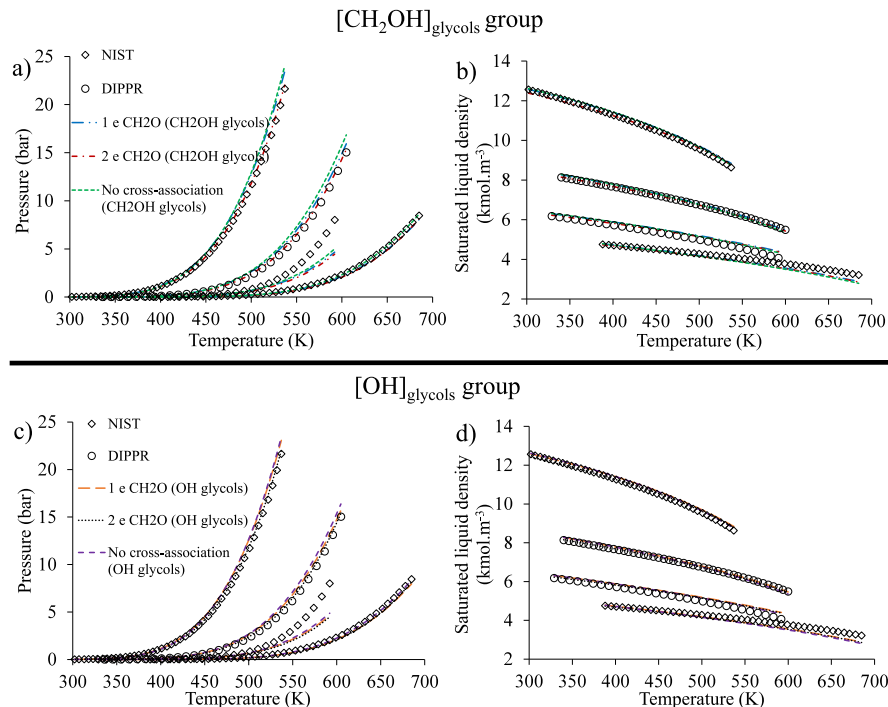


Figure 13. s-SAFT- γ Mie predictions of saturated vapor pressures (a, c) and saturated liquid densities (b, d) for the monomethyl ethers from monoethylene glycol monomethyl ether to tetraethylene glycol monomethyl ether. Results shown in (a) and (b) were obtained with the coarse-grained $[\text{CH}_2\text{OH}]_{\text{glycols}}$ group, whereas results in (c) and (d) were obtained with the $[\text{OH}]_{\text{glycols}}$ group. In parts (a) and (c), the chain length increases from left to right, whereas it increases from top to bottom in parts (b) and (d). “DIPPR” and “NIST” refer to pseudoexperimental data obtained from the DIPPR⁸⁸ and NIST⁸⁷ databases, respectively.

less suitable for use in nonaqueous alkanolamine-based carbon capture applications than shorter ones. Accordingly, the regressed s-SAFT- γ Mie parameters focus on the shorter ethylene glycols, namely, ethylene to triethylene glycol, at the expense of more general accuracy for the larger species.

Figure 12 shows binary VLE predictions for the triethylene glycol/*n*-hexane system.¹⁰⁴ Figure 12a shows results obtained with the $[\text{CH}_2\text{OH}]_{\text{glycols}}$ group, whereas Figure 12b shows results obtained with the $[\text{OH}]_{\text{glycols}}$ group. The triethylene glycol/*n*-hexane data were deemed thermodynamically inconsistent, as discussed in Section 1.3 of the Supporting Information. Therefore, this data set was omitted from the regression. Nonetheless, given the acute scarcity of the ethylene glycol/*n*-alkane VLE data in the literature, it is used for qualitative assessment of the model’s predictive capabilities.

Figure 12 shows that all the parameter sets, except for the no cross-association $[\text{OH}]_{\text{glycols}}$ parameters, accurately predict the pressure at which a liquid–liquid phase split occurs (ca. 17.2 bar). This suggests that the model captures fundamental aspects of ethylene glycol/*n*-alkane interactions, underlining its predictive capabilities for these systems.

The 2 e-site CH_2O scheme yields the least accurate results in Figure 12 (a) and (b). Moreover, the no cross-association scheme yields reduced accuracy in correlating the ethylene glycol vapor pressure, as shown in Figure 11. This suggests that the 1 e-site scheme should be carried forward in the further development of the model.

3.4. Monoalkyl Glymes. The predictive capabilities of the ethylene glycol parameters are assessed by transferring them to monoalkyl glymes.

%AAD values for s-SAFT- γ Mie predictions of the monoalkyl glyme vapor pressure and saturated liquid density are given in

Tables 8 and 9, respectively. The results shown are those obtained with the $[\text{CH}_2\text{OH}]_{\text{glycols}}$ group. Corresponding results shown for the fine-grained $[\text{OH}]_{\text{glycols}}$ group are given in Tables S6 and S7. As a visual aid to these results, s-SAFT- γ Mie predictions are illustrated in Figure 13, which shows vapor pressure and saturated liquid density results for four monomethyl ethers. Only monoalkyl glyme data for which the cited uncertainty was lower than 10% were considered for inclusion in this work.

Table 9 and Table S7 show that all considered cross-association schemes provide similar and generally accurate descriptions of monoalkyl glyme saturated liquid density with an average %AAD of ca. 2% for all schemes considered.

Figure 13 shows that s-SAFT- γ Mie provides a robust qualitative description of monoalkyl glyme vapor pressure for all schemes considered for both the $[\text{CH}_2\text{OH}]_{\text{glycols}}$ and $[\text{OH}]_{\text{glycols}}$ groups. However, Table 8 and Table S6 show that s-SAFT- γ Mie does not yield quantitatively accurate results, with average %AAD values of ca. 14–18%. The lack of quantitative accuracy echoes the results of Crespo et al.¹⁰¹ These authors investigated the transferability of SAFT- γ Mie parameters for the ethylene oxide (EO) group across several chemical families. In their work, the model required reparametrization to yield accurate descriptions of a given chemical family or even of a given system.¹⁰¹

However, it is worth noting that qualitatively meaningful predictions for a wide range of monoalkyl glymes can be obtained with the same parameter set, though no monoalkyl glymes were included in the parametrization. This underlines that the value of s-SAFT- γ Mie lies not with its accuracy but with its generalizability.

Table 8 indicates that the 2 e-site scheme provides the least accurate results, with an average vapor pressure %AAD of 17.7%. This further supports the notion that the 1 e-site scheme should be carried forward in parametrizing s-SAFT- γ Mie, as discussed in Section 3.3. The poor performance obtained with the 2-site scheme could be explained as follows: As opposed to ethylene glycols, monoalkyl glymes have only one hydroxyl group per molecule. Therefore, they may exhibit a reduced degree of association bonds relative to ethylene glycols. Accordingly, the 2 e-site scheme may well overestimate the importance of association bonds in monoalkyl glymes to the greatest extent, thereby yielding the lowest accuracy. The no cross-association and 1 e-site schemes yield similar results for monoalkyl glyme vapor pressure predictions, with average %AADs of 13.7% and 13.4%, respectively. The similarity between the no cross-association scheme and the 1 e-site scheme may indicate that the no cross-association scheme partly accounts for $\text{CH}_2\text{O}-[\text{CH}_2\text{OH}]_{\text{glycols}}([\text{OH}]_{\text{glycols}})$ cross-association in the dispersion energy. This notion is supported by the higher dispersion energy of the no cross-association $\text{CH}_2\text{O}-[\text{CH}_2\text{OH}]_{\text{glycols}}([\text{OH}]_{\text{glycols}})$ parameter sets relative to the cross-associating ones given in Table 4.

3.5. Alkanolamine/Glyme Mixtures. s-SAFT- γ Mie is further extended toward mixtures of alkanolamines with glymes. This necessitates parametrizing the CH_2NH_2 (NH_2)– CH_2O interaction. In keeping with the predictive approach taken in developing s-SAFT- γ Mie parameters, the CH_2OH (OH)– CH_2O parameters required for modeling alkanolamine/glyme mixtures are transferred from the $[\text{CH}_2\text{OH}]_{\text{glycols}}([\text{OH}]_{\text{glycols}})$ – CH_2O interaction parameters developed in Section 3.3. Only the 1 e-site CH_2O group is used, given that this group has been chosen for further use in s-SAFT- γ Mie's development.

The parameter fitting methodology developed in this work stipulates the use of binary mixture VLE in regressing interaction parameters for unlike group interactions. However, to the authors' best knowledge, no binary VLE data (i.e., $PTxy$ or Pxy data) for mixtures of alkanolamines with glymes or glycols exist. Similarly, Alkhateib et al.¹³ did not find mixture data for alkanolamines with ethylene glycols in the open literature. Though the lack of available VLE data left no other option, CH_2NH_2 (NH_2)– CH_2O parameters determined solely from alternative data types may not prove optimal for reproducing the ternary-component alkanolamine/ CO_2 /organic cosolvent phase equilibria for which the model is developed. This means that subsequently developed parameters will need to compensate for the CH_2NH_2 (NH_2)– CH_2O parameters. Therefore, should alkanolamine/glyme phase equilibria become available in the future, it may be worth revisiting the CH_2NH_2 (NH_2)– CH_2O parameters.

Fortunately, density data for mixtures of alkanolamines with glymes exist.^{91,92} However, regressing parameters solely to density data yields a very flat parameter space such that gradient-based regression algorithms fail to converge on a minimum. This issue was resolved by including excess enthalpy data for the butylamine/diethyl ether mixture⁹³ in the regression. While the CH_2NH_2 (NH_2)– CH_2O association energies thus obtained are relatively low (400–700 K), these are likely compensated for with larger association volumes (ca. 150–350 Å³).

Figures 14 and 15 show s-SAFT- γ Mie binary mixture density descriptions of monoethanolamine with monoethylene glycol monomethyl ether and with diethylene glycol dimethyl ether, respectively. For reference, the molecular structures of these glymes are listed in Figure 3.

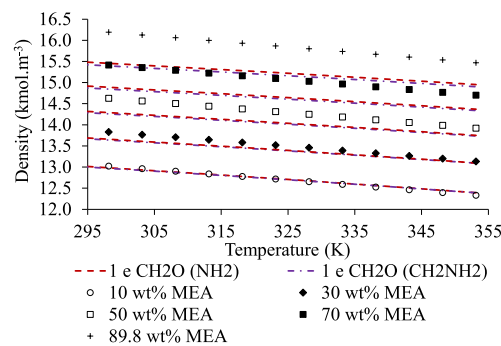


Figure 14. s-SAFT- γ Mie description of subcooled liquid density for the monoethanolamine (MEA)–monoethylene glycol monomethyl ether mixture at 1.0 bar obtained with both the fine-grained (NH_2) and coarse-grained (CH_2NH_2) groups. Experimental data are taken from Guo et al.⁹¹

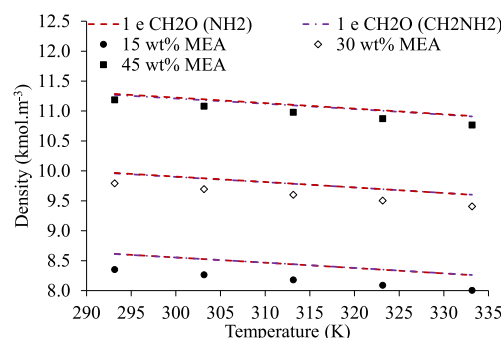


Figure 15. s-SAFT- γ Mie description of subcooled liquid density for the monoethanolamine (MEA)–diethylene glycol dimethyl ether mixture at 1 bar obtained with both the fine-grained (NH_2) and coarse-grained (CH_2NH_2) groups. Experimental data are taken from Huang et al.⁹²

Regarding the monoethanolamine/monoethylene glycol monomethyl ether system, the fitted data sets had compositions of 30 and 70 wt % monoethanolamine, respectively. The monoethanolamine/diethylene glycol dimethyl ether data sets used in the parametrization had compositions of 15 and 45 wt %. The remainder of the data sets shown in Figures 12 and 13 were left for prediction.

Figures 14 and 15 show that s-SAFT- γ Mie generally provides an accurate description of the monoethanolamine/glyme mixture density: For the binary mixture density of monoethanolamine with monoethylene glycol monomethyl ether, the %AAD is 2.1% for the CH_2NH_2 group and 2.0% for the NH_2 group. Similarly, the CH_2NH_2 group yields an %AAD of 2.0% for the mixture density of monoethanolamine with diethylene glycol dimethyl ether, whereas the NH_2 group yields an %AAD value of 2.1%. In the absence of mixture VLE data against which to assess the CH_2NH_2 (NH_2)– CH_2O parameters, these parameters are carried forward for future use in modeling ternary-component alkanolamine/ CO_2 /organic cosolvent systems.

3.6. Preliminary Caloric Property Modeling. While the discussion presented above focuses on phase equilibria, caloric properties are also relevant for the design of chemical absorption processes. The work of Oexmann and Kather¹⁰⁵ indicates that the reboiler duty of a chemical absorption process depends on the heat capacity of the carbon capture solution as well as the heat of vaporization of the cosolvent. Moreover, a consideration of caloric properties such as the heat capacity and heat of vaporization is key in determining whether a given nonaqueous

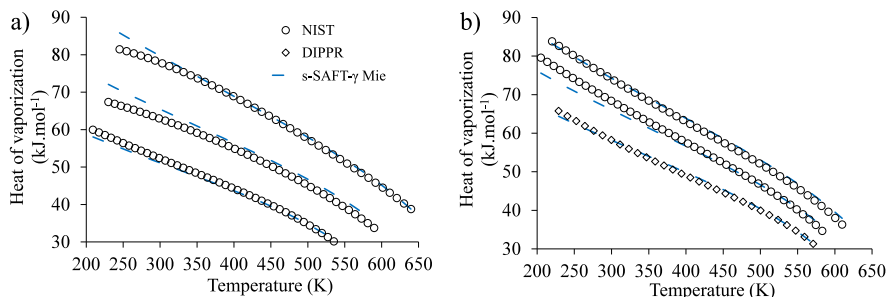


Figure 16. (a) Heats of vaporization of the dimethyl glymes from diethylene glycol dimethyl ether to tetraethylene glycol dimethyl ether predicted with s-SAFT- γ Mie. (b) Heats of vaporization of the dialkyl glymes from diethylene glycol diethyl ether to diethylene glycol dibutyl ether predicted with s-SAFT- γ Mie. The chain length increases from bottom to top. “DIPPR” and “NIST” refer to pseudoexperimental data obtained from the DIPPR⁸⁹ and NIST⁸⁷ databases, respectively.

alkanolamine promises energy savings relative to the aqueous one. Accordingly, s-SAFT- γ Mie predictions of the heat of vaporization and heat capacity for glymes and ethylene glycols are discussed in the following section.

The heat of vaporization and isobaric heat capacity data considered lie below $0.9T_c$: s-SAFT- γ Mie is developed for chemical absorption processes that operate far from critical conditions. This arguably justifies omitting the critical region from consideration in this work.

3.6.1. Heat of Vaporization. Figure 16 (a) shows the s-SAFT- γ Mie heat of vaporization predictions for dimethyl glymes. Table 6 shows that their structure is given as $\text{CH}_3-\text{[OCH}_2-\text{CH}_2\text{]}_n-\text{O-CH}_3$. The homologous series from diethylene glycol dimethyl ether to tetraethylene glycol dimethyl ether is shown. Figure 16 (b) shows the series of dialkyl glymes from diethylene glycol diethyl ether to diethylene glycol dibutyl ether. Table 6 shows that the generic structure of dialkyl glymes is $\text{CH}_3-\text{[CH}_2\text{]}_{n_1}-\text{[OCH}_2-\text{CH}_2\text{]}_{n_2}-\text{O-[CH}_2\text{]}_{n_3}-\text{CH}_3$.

For diethylene glycol diethyl ether, the data shown in Figure 16 (b) was taken from DIPPR⁸⁹ as opposed to NIST.⁸⁷ The NIST⁸⁷ data exhibited pronounced curvature when plotted as a function of temperature. This is unexpected given that the other dialkyl glymes shown in Figure 16 (b) exhibit a more linear temperature dependency. The corresponding DIPPR⁸⁹ data for diethylene glycol diethyl ether does not exhibit such unexpected curvature, arguably rendering it more suitable for use.

Figure 16 (a) shows that s-SAFT- γ Mie accurately predicts the heat of vaporization for the dimethyl glymes (the average %AAD is 2.3%). The predictions for the diethylene glycol dialkyl glymes shown in Figure 16 (b) are also quantitatively accurate (average %AAD of 1.6%). This is particularly noteworthy, given that neither of these components nor this property were included in the parametrization.

Figure 17 shows the s-SAFT- γ Mie heat of vaporization predictions for the series of ethylene glycols from monoethylene glycol to tetraethylene glycol.

The predictions for monoethylene glycol and diethylene glycol are very accurate, with an average %AAD of 2.7% obtained with the $[\text{CH}_2\text{OH}]_{\text{glycols}}$ group. However, results are less accurate for the longer-chained components tri- and tetraethylene glycol: the average %AAD is 6.3% for the $[\text{CH}_2\text{OH}]_{\text{glycols}}$ group. Results obtained with the $[\text{OH}]_{\text{glycols}}$ group are very similar. As the chain length increases, accuracy in the low-temperature region deteriorates. Notably, associative effects are stronger at lower temperatures. Accordingly, less accurate results in this region may be attributed to shortcomings in describing the association in these components. This may

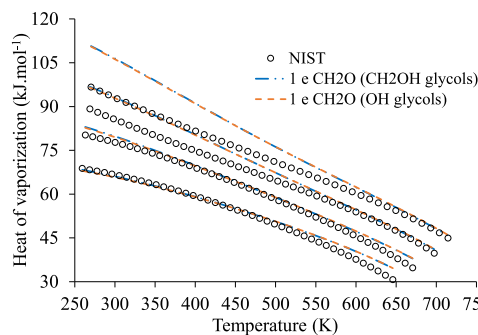


Figure 17. Heats of vaporization of monoethylene glycol to tetraethylene glycol predicted with s-SAFT- γ Mie. The chain length increases from bottom to top. Data are taken from the NIST⁸⁷ database.

suggest limits to transferring the $[\text{CH}_2\text{OH}]_{\text{glycols}}-\text{[CH}_2\text{OH}]_{\text{glycols}}([\text{OH}]_{\text{glycols}}-\text{[OH}]_{\text{glycols}})$ association interaction from monoethylene glycol to other ethylene glycols: the longer the ethylene glycol, the more the associative interactions deviate from those found in monoethylene glycol and the less suitable for use are the transferred $[\text{CH}_2\text{OH}]_{\text{glycols}}-\text{[CH}_2\text{OH}]_{\text{glycols}}([\text{OH}]_{\text{glycols}}-\text{[OH}]_{\text{glycols}})$ association parameters. Nonetheless, the overall description is robust, with an average %AAD of 4.5% for all ethylene glycols.

3.6.2. Isobaric Heat Capacity. In the following section, the discussion is extended to the isobaric heat capacity (C_p) at saturation. Only data for which the cited uncertainty is lower than 10% were included in this work. The isobaric heat capacity is determined by eq 3.

$$C_p = C_p^{IG} + C_p^{res} \quad (3)$$

While the residual contribution to the isobaric heat capacity (C_p^{res}) was computed with s-SAFT- γ Mie, the ideal contribution (C_p^{IG}) was estimated using a correlation available in the DIPPR⁸⁹ database. Notably, no C_p^{IG} correlation for diethylene glycol dipropyl ether was available. Accordingly, a correlation of the ideal gas isobaric heat capacity for this component was developed with NIST⁸⁷ data. This correlation has the same form as the one taken from the DIPPR⁸⁹ database. The correlation parameters for the ideal gas isobaric heat capacity of diethylene glycol dipropyl ether as well as the form of the correlation are given in Table S8.

Figure 18 (a) shows s-SAFT- γ Mie predictions of saturated isobaric heat capacities of the dimethyl glymes from diethylene glycol dimethyl ether to tetraethylene glycol dimethyl ether. The

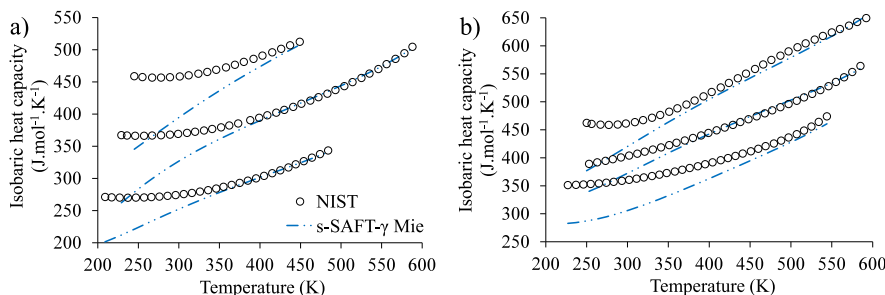


Figure 18. (a) Saturated isobaric heat capacities of the dimethyl glymes from diethylene glycol dimethyl ether to tetraethylene glycol dimethyl ether predicted with s-SAFT- γ Mie. (b) Saturated isobaric heat capacities of the dialkyl glymes from diethylene glycol diethyl ether to diethylene glycol dibutyl ether obtained with s-SAFT- γ Mie. The chain length increases from bottom to top. Data are taken from the NIST⁸⁷ database.

series of dialkyl glymes from diethylene glycol diethyl ether to diethylene glycol dibutyl ether is shown in Figure 18 (b).

Overall, Figure 18 shows that s-SAFT- γ Mie provides robust predictions of dialkyl glyme saturated isobaric heat capacity with an average %AAD of 6.5% for all species considered. Predictions are less accurate for lower temperatures. However, s-SAFT- γ Mie was not parametrized at very low temperatures (below 50% of the critical temperature ($0.5T_c$)). This may in part account for the poor performance in the low-temperature region. Moreover, the reduced accuracy in the low-temperature region may indicate that components featuring repeating groups pose a challenge to the model, as discussed in Section 3.1.2.

Figure 19 provides s-SAFT- γ Mie saturated isobaric heat capacity predictions for the homologous series of ethylene glycols from monoethylene glycol to tetraethylene glycol.

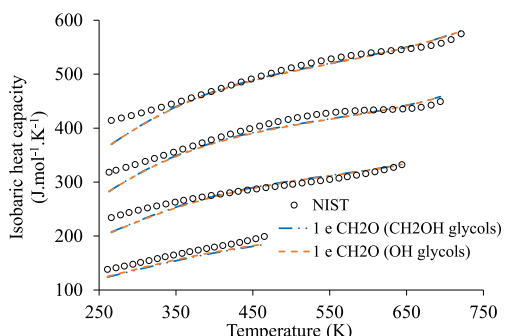


Figure 19. Saturated isobaric heat capacities of monoethylene glycol to tetraethylene glycol predicted with s-SAFT- γ Mie. The chain length increases from bottom to top. Data are taken from the NIST⁸⁷ database.

Figure 19 shows that s-SAFT- γ Mie provides good quantitative predictions of the saturated isobaric heat capacity of the ethylene glycols from diethylene glycol to tetraethylene glycol (average %AAD of 2.6%). As for the dialkyl glymes (Figure 18), the reduced accuracy at lower temperatures may again be partially attributable to the fact that s-SAFT- γ Mie was not parametrized below $0.5T_c$.

However, s-SAFT- γ Mie consistently underestimates the heat capacity of monoethylene glycol, yielding a %AAD of 7.3% for this component. The work of Cerdeirinha et al.¹⁰⁶ indicates that the pure-component liquid-phase isobaric heat capacity is governed by the association energy, the molecules' capability to associate, and the molecular size. Accordingly, poor descriptions of the isobaric heat capacity may indicate a shortcoming in s-SAFT- γ Mie's description of complex associative effects in pure monoethylene glycol. Notably,

hydrogen bond cooperativity is neglected in SAFT EoSs.¹⁰⁷ As discussed in previous work,⁸⁰ there is evidence for cooperative effects in pure glycerol,¹⁰⁸ another simple polyalcohol. Accordingly, it is plausible that such effects are present in monoethylene glycol and that they should be accounted for in modeling this component.

Overall, however, s-SAFT- γ Mie provides a good description of the saturated liquid phase isobaric heat capacity of ethylene glycols, with an average %AAD of 3.8% for all ethylene glycols considered. s-SAFT- γ Mie's performance in modeling both the heat of vaporization and the isobaric heat capacity indicates that the EoSs predictive capabilities extend beyond phase equilibria to caloric properties. This further underlines the value of s-SAFT- γ Mie in preliminary process design for nonaqueous alkanolamine-based carbon capture processes.

4. CONCLUSIONS

A continuation of previous work,⁸⁰ this work entailed further developing the s-SAFT- γ Mie EoS toward a description of ternary-component nonaqueous alkanolamine-based carbon capture systems. This parametrization was performed according to a consistent and systematic methodology, thereby providing an example of how group-contribution EoSs can be parametrized in the context of nonaqueous alkanolamine-based carbon capture systems. It is hoped that this will provide industrial practitioners with a useful framework for developing similar models in the context of the alkanolamine-based carbon capture space.

Group interaction parameters were developed for ethylene glycols as well as mono- and dialkyl glymes. At this advanced stage of model development, limitations became apparent: It was found that the primary alcohol (CH₂OH/OH) group could not quantitatively describe the vapor pressure of monoethylene glycol, necessitating a unique ethylene glycol hydroxyl group ([CH₂OH]_{glycols}/[OH]_{glycols}). This provides evidence of the trade-off inherent in group-contribution modeling with s-SAFT- γ Mie: its ability to provide predictions for a wide range of systems with a single parameter set comes at the cost of quantitatively accurate predictions.

The [CH₂OH]_{glycols}/[OH]_{glycols} parameters were subsequently transferred to ethylene glycols, which also feature the ether (CH₂O) group. A 1 e-site association scheme was chosen for the CH₂O group. This accounts for [CH₂OH]_{glycols}/[OH]_{glycols}–CH₂O group cross-association, thereby resulting in a more physically meaningful model.

s-SAFT- γ Mie provided accurate pure-component phase equilibria descriptions of shorter ethylene glycols, yielding an average vapor pressure %AAD of 2.8% (2.9% with the [OH]_{glycols}

group) with the 1 e-site CH_2O scheme. Moreover, the model correctly identified the existence of a liquid–liquid phase split in the triethylene glycol/n-hexane system. For longer ethylene glycols, mono- and diethers, as well as mono- and dialkyl glymes, the predictions were not quantitative. The predicted dialkyl glyme vapor pressure %AAD was 10.4%. For the monoalkyl glymes, the average vapor pressure %AAD obtained with the 1 e-site CH_2O scheme was 13.4% (13.1% with the $[\text{OH}]_{\text{glycols}}$ group). Nonetheless, it is stressed that the results were qualitatively accurate. These results indicate that s-SAFT- γ Mie captures fundamental aspects of this wide range of systems using the same set of transferable group interaction parameters throughout. This highlights s-SAFT- γ Mie's value in the preliminary design of alkanolamine-based carbon capture processes, where rapidly obtainable and qualitative property estimates for a given component may be preferred to time- and resource-intensive experimental measurement.

Finally, s-SAFT- γ Mie proved to have robust predictive capabilities for heat of vaporization and saturated isobaric heat capacities of pure dialkyl glymes and ethylene glycols. For the ethylene glycols, the average %AADs were 4.5 and 1.6% for the dialkyl glymes not included in the parametrization. Regarding the saturated isobaric heat capacity, the average %AAD was 3.8% for the ethylene glycols and 6.5% for the dialkyl glymes. These results indicate that s-SAFT- γ Mie's predictive capabilities also hold for calorific properties. This further illustrates the model's value as a tool for the preliminary design of alkanolamine-based carbon capture processes.

ASSOCIATED CONTENT

Supporting Information

The Supporting Information is available free of charge at <https://pubs.acs.org/doi/10.1021/acs.iecr.4c00090>.

s-SAFT- γ Mie *a priori* structural parameters; additional s-SAFT- γ Mie descriptions of monoalkyl glyme vapor pressure and saturated liquid density obtained using the $[\text{OH}]_{\text{glycols}}$ group; details of correlation used to determine the ideal gas isobaric heat capacity of diethylene glycol dipropyl ether; discussion of thermodynamic consistency tests employed in this work; and a discussion of thermodynamic consistency testing results of binary VLE data chosen for regression ([PDF](#))

AUTHOR INFORMATION

Corresponding Author

Jamie T. Cripwell – Department of Chemical Engineering, Stellenbosch University, Matieland 7602, South Africa; orcid.org/0000-0002-2439-5460; Email: cripwell@sun.ac.za

Authors

Alexander Schulze-Hulbe – Department of Chemical Engineering, Stellenbosch University, Matieland 7602, South Africa; orcid.org/0000-0002-7935-8958

Andries J. Burger – Department of Chemical Engineering, Stellenbosch University, Matieland 7602, South Africa; orcid.org/0000-0001-6588-807X

Complete contact information is available at:

<https://pubs.acs.org/10.1021/acs.iecr.4c00090>

Notes

The authors declare no competing financial interest.

ACKNOWLEDGMENTS

The financial assistance of Sasol Technology (Pty) Ltd. as well as the Wilhelm Frank foundation is hereby acknowledged. Opinions expressed and conclusions presented are those of the authors and are not necessarily to be attributed to the sponsors.

REFERENCES

- (1) MacDowell, N.; Florin, N.; Buchard, A.; Hallett, J.; Galindo, A.; Jackson, G.; Adjiman, C. S.; Williams, C. K.; Shah, N.; Fennell, P. An Overview of CO_2 Capture Technologies. *Energy Environ. Sci.* **2010**, *3* (11), 1645–69.
- (2) Benhelal, E.; Zahedi, G.; Shamsaei, E.; Bahadori, A. Global Strategies and Potentials to Curb CO_2 Emissions in Cement Industry. *J. Cleaner Prod.* **2013**, *51*, 142–61.
- (3) Bui, M.; Adjiman, C. S.; Bardow, A.; Anthony, E. J.; Boston, A.; Brown, S.; Fennell, P. S.; Fuss, S.; Galindo, A.; Hackett, L. A.; et al. Carbon Capture and Storage (CCS): The Way Forward. *Energy Environ. Sci.* **2018**, *11* (5), 1062–176.
- (4) Vrbová, V.; Ciahotný, K. Upgrading Biogas to Biomethane Using Membrane Separation. *Energy Fuels* **2017**, *31* (9), 9393–401.
- (5) Liang, Z. H.; Rongwong, W.; Liu, H.; Fu, K.; Gao, H.; Cao, F.; Zhang, R.; Sema, T.; Henni, A.; Sumon, K.; et al. Recent Progress and New Developments in Post-Combustion Carbon-Capture Technology with Amine Based Solvents. *Int. J. Greenh. Gas Control* **2015**, *40*, 26–54.
- (6) Liang, Z.; Fu, K.; Idem, R.; Tontiwachwuthikul, P. Review on Current Advances, Future Challenges and Consideration Issues for Post-Combustion CO_2 Capture Using Amine-Based Absorbents. *Chin. J. Chem. Eng.* **2016**, *24* (2), 278–88.
- (7) Mondal, M. K.; Balsora, H. K.; Varshney, P. Progress and Trends in CO_2 Capture/Separation Technologies: A Review. *Energy* **2012**, *46* (1), 431–41.
- (8) Heldebrant, D. J.; Koech, P. K.; Glezakou, V. A.; Rousseau, R.; Malhotra, D.; Cantu, D. C. Water-Lean Solvents for Post-Combustion CO_2 Capture: Fundamentals, Uncertainties, Opportunities, and Outlook. *Chem. Rev.* **2017**, *117* (14), 9594–624.
- (9) Vitillo, J. G.; Smit, B.; Gagliardi, L. Introduction: Carbon Capture and Separation. *Chem. Rev.* **2017**, *117* (14), 9521–3.
- (10) Budzianowski, W. M. Explorative Analysis of Advanced Solvent Processes for Energy Efficient Carbon Dioxide Capture by Gas-Liquid Absorption. *Int. J. Greenh. Gas Control* **2016**, *49*, 108–20.
- (11) Chowdhury, F. A.; Goto, K.; Yamada, H.; Matsuzaki, Y. A Screening Study of Alcohol Solvents for Alkanolamine-Based CO_2 Capture. *Int. J. Greenh. Gas Control* **2020**, *99*, No. 103081.
- (12) Bahamon, D.; Alkhatab, I. I. I.; Alkhatab, N.; Builes, S.; Sinnokrot, M.; Vega, L. F. A Comparative Assessment of Emerging Solvents and Adsorbents for Mitigating CO_2 Emissions from the Industrial Sector by Using Molecular Modeling Tools. *Front. Energy Res.* **2020**, *8*, 00165.
- (13) Alkhatab, I. I. I.; Pereira, L. M. C.; Alhajaj, A.; Vega, L. F. Performance of Non-Aqueous Amine Hybrid Solvent Mixtures for CO_2 Capture: A Study Using a Molecular-based Model. *J. CO₂ Util.* **2020**, *35*, 126–144.
- (14) Wanderley, R. R.; Pinto, D. D. D.; Knuutila, H. K. From Hybrid Solvents to Water-Lean Solvents – A Critical and Historical Review. *Sep. Purif. Technol.* **2021**, *260*, No. 118193.
- (15) Barzaghi, F.; Mani, F.; Peruzzini, M. Efficient CO_2 Absorption and Low Temperature Desorption with Non-Aqueous Solvents Based on 2-Amino-2-Methyl-1-Propanol (AMP). *Int. J. Greenh. Gas Control* **2013**, *16*, 217–23.
- (16) Barzaghi, F.; Lai, S.; Mani, F.; Stopponi, P. Novel Non-Aqueous Amine Solvents for Biogas Upgrading. *Energy Fuels* **2014**, *28*, 5252–8.
- (17) Barbarossa, V.; Barzaghi, F.; Mani, F.; Lai, S. Efficient CO_2 Capture by Non-Aqueous 2-Amino-2-Methyl-1-Propanol (AMP) and Low Temperature Solvent Regeneration. *RSC Adv.* **2013**, *3*, 12349–12355.
- (18) Mathias, P. M.; Afshar, K.; Zheng, F.; Bearden, M. D.; Freeman, C. J.; Andrea, T.; Koech, P. K.; Kutnyakov, I.; Zwoster, A.; Smith, A. R.;

- et al. Improving the Regeneration of CO₂-Binding Organic Liquids with a Polarity Change. *Energy Environ. Sci.* **2013**, *6* (7), 2233–42.
- (19) Guo, H.; Li, C.; Shi, X.; Li, H.; Shen, S. Nonaqueous Amine-Based Absorbents for Energy Efficient CO₂ Capture. *Appl. Energy* **2019**, *239*, 725–34.
- (20) Yuan, Y.; Rochelle, G. T. CO₂ Absorption Rate in Semi-Aqueous Monoethanolamine. *Chem. Eng. Sci.* **2018**, *182*, 56–66.
- (21) Barzaghi, F.; Giorgi, C.; Mani, F.; Peruzzini, M. Reversible Carbon Dioxide Capture by Aqueous and Non-Aqueous Amine-Based Absorbents: A Comparative Analysis Carried out by ¹³C NMR Spectroscopy. *Appl. Energy* **2018**, *220*, 208–19.
- (22) Tan, Y.; Nookuea, W.; Li, H.; Thorin, E.; Yan, J. Property Impacts on Carbon Capture and Storage (CCS) Processes: A Review. *Energy Convers. Manag.* **2016**, *118*, 204–22.
- (23) Wertheim, M. Fluids with Highly Directional Attractive Forces. I. Statistical Thermodynamics. *J. Stat. Phys.* **1984**, *35* (1–2), 19–34.
- (24) Wertheim, M. Fluids with Highly Directional Attractive Forces. II. Thermodynamic Perturbation Theory and Integral Equations. *J. Stat. Phys.* **1984**, *35* (1–2), 35–47.
- (25) Wertheim, M. Fluids with Highly Directional Attractive Forces. III. Multiple Attraction Sites. *J. Stat. Phys.* **1986**, *42* (3–4), 459–76.
- (26) Wertheim, M. Fluids with Highly Directional Attractive Forces. IV. Equilibrium Polymerization. *J. Stat. Phys.* **1986**, *42* (3–4), 477–92.
- (27) Li, X. S.; Englezos, P. Vapor-Liquid Equilibrium of Systems Containing Alcohols, Water, Carbon Dioxide and Hydrocarbons Using SAFT. *Fluid Phase Equilib.* **2004**, *224* (1), 111–8.
- (28) Gross, J.; Sadowski, G. Application of the Perturbed-Chain SAFT Equation of State to Associating Systems. *Ind. Eng. Chem. Res.* **2002**, *41*, 5510–5.
- (29) Papaioannou, V.; Adjiman, C. S.; Jackson, G.; Galindo, A. Simultaneous Prediction of Vapour-Liquid and Liquid-Liquid Equilibria (VLE and LLE) of Aqueous Mixtures with the SAFT- γ Group Contribution Approach. *Fluid Phase Equilib.* **2011**, *306* (1), 82–96.
- (30) Liang, X.; Tsivitzelis, I.; Kontogeorgis, G. M. Modeling Water Containing Systems with the Simplified PC-SAFT and CPA Equations of State. *Ind. Eng. Chem. Res.* **2014**, *53* (37), 14493–507.
- (31) Cripwell, J.; Smith, S. A. M.; Schwarz, C. E.; Burger, A. J. SAFT-VR Mie: Applications to Phase Equilibria of Alcohols in Mixtures with n-Alkanes and Water. *Ind. Eng. Chem. Res.* **2018**, *57* (29), 9693–706.
- (32) Tumakaka, F.; Gross, J.; Sadowski, G. Modeling of Polymer Phase Equilibria using Perturbed-Chain SAFT. *Fluid Phase Equilib.* **2002**, *194*–197, 541–51.
- (33) Kouskoumvekaki, I. A.; von Solms, N.; Michelsen, M. L.; Kontogeorgis, G. M. Application of the Perturbed Chain SAFT Equation of State to Complex Polymer Systems using Simplified Mixing Rules. *Fluid Phase Equilib.* **2004**, *215*, 71–8.
- (34) Kouskoumvekaki, I. A.; von Solms, N.; Lindvig, T.; Michelsen, M. L.; Kontogeorgis, G. M. Novel Method for Estimating Pure-Component Parameters for Polymers: Application to the PC-SAFT Equation of State. *Ind. Eng. Chem. Res.* **2004**, *43* (11), 2830–8.
- (35) von Solms, N.; Michelsen, M. L.; Kontogeorgis, G. M. Prediction and Correlation of High-Pressure Gas Solubility in Polymers with Simplified PC-SAFT. *Ind. Eng. Chem. Res.* **2005**, *44* (9), 3330–5.
- (36) Peters, F. T.; Laube, F. S.; Sadowski, G. Development of a Group Contribution Method for Polymers within the PC-SAFT Model. *Fluid Phase Equilib.* **2012**, *324*, 70–9.
- (37) Tibic, A.; Kontogeorgis, G. M.; von Solms, N.; Michelsen, M. L. A Predictive Group-Contribution Simplified PC-SAFT Equation of State: Application to Polymer Systems. *Ind. Eng. Chem. Res.* **2008**, *47* (15), 5092–5101.
- (38) Pedrosa, N.; Vega, L. F.; Coutinho, J. A. P.; Marrucho, I. M. Phase Equilibria Calculations of Polyethylene Solutions from SAFT-Type Equations of State. *Macromolecules* **2006**, *39* (12), 4240–6.
- (39) Tibic, A.; von Solms, N.; Michelsen, M. L.; Kontogeorgis, G. M.; Constantinou, L. Application of sPC-SAFT and Group Contribution sPC-SAFT to Polymer Systems - Capabilities and Limitations. *Fluid Phase Equilib.* **2009**, *281*, 70–7.
- (40) Cameretti, L. F.; Sadowski, G.; Møllerup, J. M. Modeling of Aqueous Electrolyte Solutions with Perturbed-Chain Statistical Associated Fluid Theory. *Ind. Eng. Chem. Res.* **2005**, *44* (9), 3355–62.
- (41) Held, C.; Reschke, T.; Mohammad, S.; Luza, A.; Sadowski, G. ePC-SAFT Revised. *Chem. Eng. Res. Des.* **2014**, *92* (12), 2884–97.
- (42) Held, C.; Reschke, T.; Müller, R.; Kunz, W.; Sadowski, G. Measuring and Modeling Aqueous Electrolyte/Amino-Acid Solutions with ePC-SAFT. *J. Chem. Thermodyn.* **2014**, *68*, 1–12.
- (43) Mohammad, S.; Grundl, G.; Müller, R.; Kunz, W.; Sadowski, G.; Held, C. Influence of Electrolytes on Liquid-Liquid Equilibria of Water/1-Butanol and on the Partitioning of 5-Hydroxymethylfurfural in Water/1-Butanol. *Fluid Phase Equilib.* **2016**, *428*, 102–11.
- (44) Pabsch, D.; Held, C.; Sadowski, G. Modeling the CO₂ Solubility in Aqueous Electrolyte Solutions Using ePC-SAFT. *J. Chem. Eng. Data* **2020**, *65* (12), 5768–77.
- (45) Llovel, F.; Marcos, R. M.; MacDowell, N.; Vega, L. F. Modeling the Absorption of Weak Electrolytes and Acid Gases with Ionic Liquids Using the Soft-SAFT Approach. *J. Phys. Chem. B* **2012**, *116* (26), 7709–18.
- (46) Galindo, A.; Gil-Villegas, A.; Jackson, G.; Burgess, A. N. SAFT-VRE: Phase Behavior of Electrolyte Solutions with the Statistical Associating Fluid Theory for Potentials of Variable Range. *J. Phys. Chem. B* **1999**, *103* (46), 10272–81.
- (47) Gil-Villegas, A.; Galindo, A.; Jackson, G. A Statistical Associating Fluid Theory for Electrolyte Solutions (SAFT-VRE). *Mol. Phys.* **2001**, *99* (6), 531–46.
- (48) Kontogeorgis, G. M.; Folas, G. *Thermodynamic Models for Industrial Applications*; John Wiley and Sons: Chichester: U.K., 2010.
- (49) Müller, E. A.; Gubbins, K. E. Molecular-Based Equations of State for Associating Fluids: A Review of SAFT and Related Approaches. *Ind. Eng. Chem. Res.* **2001**, *40* (10), 2193–211.
- (50) Tan, S.; Adidharma, H.; Radosz, M. Recent Advances and Applications of Statistical Associating Fluid Theory. *Ind. Eng. Chem. Res.* **2008**, *47* (21), 8063–82.
- (51) Diamantonis, N. I.; Economou, I. G. Evaluation of Statistical Associating Fluid Theory (SAFT) and Perturbed Chain-SAFT Equations of State for the Calculation of Thermodynamic Derivative Properties of Fluids Related to Carbon Capture and Sequestration. *Energy Fuels* **2011**, *25* (7), 3334–43.
- (52) Diamantonis, N. I.; Boulougouris, G. C.; Mansoor, E.; Tsangaris, D. M.; Economou, I. G. Evaluation of Cubic, SAFT, and PC-SAFT Equations of State for the Vapor-liquid Equilibrium Modeling of CO₂ Mixtures with other Gases. *Ind. Eng. Chem. Res.* **2013**, *52* (10), 3933–42.
- (53) Perez, A. G.; Coquelet, C.; Paricaud, P.; Chapoy, A. Comparative Study of Vapour-Liquid Equilibrium and Density Modelling of Mixtures Related to Carbon Capture and Storage with the SRK, PR, PC-SAFT and SAFT-VR Mie Equations of State for Industrial Uses. *Fluid Phase Equilib.* **2017**, *440*, 19–35.
- (54) Chremos, A.; Forte, E.; Papaioannou, V.; Galindo, A.; Jackson, G.; Adjiman, C. S. Modelling the Phase and Chemical Equilibria of Aqueous Solutions of Alkanolamines and Carbon Dioxide using the SAFT- γ SW Group Contribution Approach. *Fluid Phase Equilib.* **2016**, *407*, 280–97.
- (55) Khalit, S. H. Development of SAFT- γ Mie Models for Alkanolamines for Carbon Capture Studies. Ph.D. Thesis, Imperial College London, London, U.K., 2019.
- (56) Najafloo, A.; Zarei, S. Modeling Solubility of CO₂ in Aqueous Monoethanolamine (MEA) Solution using SAFT-HR Equation of State. *Fluid Phase Equilib.* **2018**, *456*, 25–32.
- (57) Pereira, L. M. C.; Llovel, F.; Vega, L. F. Thermodynamic Characterisation of Aqueous Alkanolamine and Amine Solutions for Acid Gas Processing by Transferable Molecular Models. *Appl. Energy* **2018**, *222*, 687–703.
- (58) Pereira, L. M. C.; Vega, L. F. A Systematic Approach for the Thermodynamic Modelling of CO₂-Amine Absorption Process using Molecular-Based Models. *Appl. Energy* **2018**, *232*, 273–91.

- (59) Lloret, J. O.; Vega, L. F.; Llovell, F. A Consistent and Transferable Thermodynamic Model to Accurately Describe CO₂ Capture with Monoethanolamine. *J. CO₂ Util.* **2017**, *21*, 521–533.
- (60) Mac Dowell, N.; Llovell, F.; Adjiman, C. S.; Jackson, G.; Galindo, A. Modeling the Fluid Phase Behavior of Carbon Dioxide in Aqueous Solutions of Monoethanolamine Using Transferable Parameters with the SAFT-VR Approach. *Ind. Eng. Chem. Res.* **2010**, *49* (4), 1883–99.
- (61) Mac Dowell, N.; Pereira, F. E.; Llovell, F.; Blas, F. J.; Adjiman, C. S.; Jackson, G.; Galindo, A. Transferable SAFT-VR Models for the Calculation of the Fluid Phase Equilibria in Reactive Mixtures of Carbon Dioxide, Water, and n-Alkylamines in the Context of Carbon Capture. *J. Phys. Chem. B* **2011**, *115* (25), 8155–68.
- (62) Rodriguez, J.; Mac Dowell, N.; Llovell, F.; Adjiman, C. S.; Jackson, G.; Galindo, A. Modelling the Fluid Phase Behaviour of Aqueous Mixtures of Multifunctional Alkanolamines and Carbon Dioxide Using Transferable Parameters with the SAFT-VR Approach. *Mol. Phys.* **2012**, *110* (11–12), 1325–48.
- (63) Pahlavanzadeh, H.; Fakouri Baygi, S. Modeling CO₂ Solubility in Aqueous Methylidiethanolamine Solutions by Perturbed Chain-SAFT Equation of State. *J. Chem. Thermodyn.* **2013**, *59*, 214–21.
- (64) Fakouri Baygi, S.; Pahlavanzadeh, H. Application of the Perturbed Chain-SAFT Equation of State for Modeling CO₂ Solubility in Aqueous Monoethanolamine Solutions. *Chem. Eng. Res. Des.* **2015**, *93*, 789–99.
- (65) Najafloo, A.; Feyzi, F.; Zoghi, A. T. Modeling Solubility of CO₂ in Aqueous MDEA Solution Using Electrolyte SAFT-HR EoS. *J. Taiwan Inst. Chem. Eng.* **2016**, *58*, 381–90.
- (66) Huang, S.; Radosz, M. Equation of State for Small, Large, Polydisperse and Associating Molecules. *Ind. Eng. Chem. Res.* **1990**, *29* (11), 2284–94.
- (67) Gross, J.; Sadowski, G. Perturbed-Chain SAFT: An Equation of State Based on a Perturbation Theory for Chain Molecules. *Ind. Eng. Chem. Res.* **2001**, *40* (4), 1244–60.
- (68) von Solms, N.; Michelsen, M. L.; Kontogeorgis, G. M. Computational and Physical Performance of a Modified PC-SAFT Equation of State for Highly Asymmetric and Associating Mixtures. *Ind. Eng. Chem. Res.* **2003**, *42* (5), 1098–105.
- (69) Papaioannou, V.; Lafitte, T.; Avendaño, C.; Adjiman, C. S.; Jackson, G.; Müller, E. A.; Galindo, A. Group Contribution Methodology Based on the Statistical Associating Fluid Theory for Heteronuclear Molecules Formed from Mie Segments. *J. Chem. Phys.* **2014**, *140* (5), No. 054107.
- (70) Lafitte, T.; Apostolakou, A.; Avendaño, C.; Galindo, A.; Adjiman, C. S.; Müller, E. A.; Jackson, G. Accurate Statistical Associating Fluid Theory for Chain Molecules Formed from Mie Segments. *J. Chem. Phys.* **2013**, *139* (15), No. 154504.
- (71) Lafitte, T.; Bessieres, D.; Piñeiro, M. M.; Daridon, J. L. Simultaneous Estimation of Phase Behavior and Second-Derivative Properties Using the Statistical Associating Fluid Theory with Variable Range Approach. *J. Chem. Phys.* **2006**, *124* (2), No. 024509.
- (72) Lafitte, T.; Piñeiro, M. M.; Daridon, J. L.; Bessières, D. A Comprehensive Description of Chemical Association Effects on Second Derivative Properties of Alcohols Through a SAFT-VR Approach. *J. Phys. Chem. B* **2007**, *111* (13), 3447–61.
- (73) Zhu, C.; Liu, X.; He, M.; Kontogeorgis, G. M.; Liang, X. Heat Capacities of Fluids: The Performance of Various Equations of State. *J. Chem. Eng. Data* **2020**, *65* (12), 5654–76.
- (74) Haslam, A. J.; González-Pérez, A.; Di Lecce, S.; Khalit, S. H.; Perdomo, F. A.; Kournopoulos, S.; Kohns, M.; Lindeboom, T.; Wehbe, M.; Febra, S.; et al. Expanding the Applications of the SAFT- γ Mie Group-Contribution Equation of State: Prediction of Thermodynamic Properties and Phase Behavior of Mixtures. *J. Chem. Eng. Data* **2020**, *65* (12), 5862–90.
- (75) Hutacharoen, P.; Dufal, S.; Papaioannou, V.; Shanker, R. M.; Adjiman, C. S.; Jackson, G.; Galindo, A. Predicting the Solvation of Organic Compounds in Aqueous Environments: From Alkanes and Alcohols to Pharmaceuticals. *Ind. Eng. Chem. Res.* **2017**, *56* (38), 10856–76.
- (76) Febra, S. A.; Bernet, T.; Mack, C.; McGinty, J.; Onyemelukwe, I. I.; Urwin, S. J.; Sefcik, J.; ter Horst, J. H.; Adjiman, C. S.; Jackson, G.; et al. Extending the SAFT- γ Mie Approach to Model Benzoic Acid, Diphenylamine, and Mefenamic Acid: Solubility Prediction and Experimental Measurement. *Fluid Phase Equilib.* **2021**, *540*, No. 113002.
- (77) Perdomo, F. A.; Khalit, S. H.; Graham, E. J.; Tzirakis, F.; Papadopoulos, A. I.; Tsivintzelis, I.; Seferlis, P.; Adjiman, C. S.; Jackson, G.; Galindo, A. A Predictive Group Contribution Framework for the Thermodynamic Modelling of CO₂ Absorption in Cyclic Amines, Alkyl Polyamines, Alkanolamines and Phase-change Amines: New Data and SAFT- γ Mie Parameters. *Fluid Phase Equilib.* **2023**, *566*, No. 113635.
- (78) Shaahmadi, F.; Hurter, R. M.; Cripwell, J. T.; Burger, A. J. Improving the SAFT- γ Mie Equation of State to Account for Functional Group Interactions in a Structural (s-SAFT- γ Mie) Framework: Linear & Branched Alkanes. *J. Chem. Phys.* **2021**, *154* (24), No. 244102.
- (79) Schulze-Hulbe, A.; Shaahmadi, F.; Burger, A. J.; Cripwell, J. T. Extending the Structural (s)-SAFT- γ Mie Equation of State to Primary Alcohols. *Ind. Eng. Chem. Res.* **2022**, *61* (33), 12208–28.
- (80) Schulze-Hulbe, A.; Shaahmadi, F.; Burger, A. J.; Cripwell, J. T. Toward Nonaqueous Alkanolamine-Based Carbon Capture Systems: Parameterizing Amines, Secondary Alcohols, and Carbon Dioxide-Containing Systems in s-SAFT- γ Mie. *Ind. Eng. Chem. Res.* **2023**, *62* (35), 14061–83.
- (81) Papadopoulos, A. I.; Badr, S.; Chremos, A.; Forte, E.; Zarogiannis, T.; Seferlis, P.; Papadokonstantakis, S.; Galindo, A.; Jackson, G.; Adjiman, C. S. Computer-Aided Molecular Design and Selection of CO₂ Capture Solvents Based on Thermodynamics, Reactivity and Sustainability. *Mol. Syst. Des. Eng.* **2016**, *1* (3), 313–34.
- (82) Papadopoulos, A. I.; Perdomo, F. A.; Tzirakis, F.; Shavalieva, G.; Tsivintzelis, I.; Kazepidis, P.; Nessi, E.; Papadokonstantakis, S.; Seferlis, P.; Galindo, A.; et al. Molecular Engineering of Sustainable Phase-Change Solvents: From Digital Design to Scaling-Up for CO₂ Capture. *Chem. Eng. J.* **2021**, *420*, No. 127624.
- (83) Alkhatab, I. I. I.; Khalifa, O.; Bahamom, D.; Abu-Zahra, M. R. M.; Vega, L. F. Sustainability Criteria as a Game Changer in the Search for Hybrid Solvents for CO₂ and H₂S Removal. *Sep. Purif. Technol.* **2021**, *277*, No. 119516.
- (84) Alkhatab, I. I. I.; Galindo, A.; Vega, L. F. Systematic Study of the Effect of the Co-Solvent on the Performance of Amine-based Solvents for CO₂ Capture. *Sep. Purif. Technol.* **2022**, *282*, No. 120093.
- (85) Ameen, J.; Furbush, S. A. Solvent Composition Useful in Acid Gas Removal from Gas Mixtures; 1973, US3737392.
- (86) Kontogeorgis, G. M.; Dohrn, R.; Economou, I. G.; de Hemptinne, J. C.; ten Kate, A.; Kuitunen, S.; Mooijer, M.; Zilnik, L. F.; Vesovic, V. Industrial Requirements for Thermodynamic and Transport Properties: 2020. *Ind. Eng. Chem. Res.* **2021**, *60* (13), 4987–5013.
- (87) Diky, V.; Muzny, C.; Smolyanitsky, A.; Bazyleva, A.; Chirico, R.; Magee, J.; Paulechka, Y.; Kazakov, A.; Townsend, S.; Lemmon, E.; et al. *ThermoData Engine (TDE) (Pure Compounds, Binary Mixtures, Ternary Mixtures, and Chemical Reactions): NIST Standard Reference Database 103b*, version 10.1; National Institute of Standards and Technology, Standard Reference Program: Gaithersburg, MD, 2016.
- (88) Wilding, W. V.; Knotts, T. A.; Giles, N. F.; Rowley, R. L. *DIPPR Data Compilation of Pure Chemical Properties*; Design Institute for Physical Properties, AIChE: New York, 2020.
- (89) Wilding, W. V.; Knotts, T. A.; Giles, N. F.; Rowley, R. L. *DIPPR Data Compilation of Pure Chemical Properties*; Design Institute for Physical Properties, AIChE: New York, 2022.
- (90) Treszczanowicz, T.; C.-Y. Lu, B. (Vapour + Liquid) Equilibria of (3,6-Dioxaoctane + n-Heptane) at 343.15 K. *J. Chem. Thermodyn.* **1987**, *19* (4), 391–394.
- (91) Guo, H.; Hui, L.; Shen, S. Monoethanolamine+2-Methoxyethanol Mixtures for CO₂ Capture: Density, Viscosity and CO₂ Solubility. *J. Chem. Thermodyn.* **2019**, *132*, 155–63.
- (92) Huang, W.; Mi, Y.; Li, Y.; Zheng, D. An Aprotic Polar Solvent, Diglyme, Combined with Monoethanolamine to Form CO₂ Capture

- Material: Solubility Measurement, Model Correlation, and Effect Evaluation. *Ind. Eng. Chem. Res.* **2015**, *54* (13), 3430–3437.
- (93) Letcher, T. M.; Goldon, A. Excess Molar Enthalpies of (Butylamine + an Ether) at 298.15 K. *J. Chem. Eng. Data* **1996**, *41* (3), 629–633.
- (94) Valderrama, J. O.; Alvarez, V. H. A Versatile Thermodynamic Consistency Test for Incomplete Phase Equilibrium Data of High-Pressure Gas-Liquid Mixtures. *Fluid Phase Equilib.* **2004**, *226*, 149–159.
- (95) Burger, J.; Papaioannou, V.; Gopinath, S.; Jackson, G.; Galindo, A.; Adjiman, C. S. A Hierarchical Method to Integrated Solvent and Process Design of Physical CO₂ Absorption Using the SAFT- γ Mie Approach. *AICHE J.* **2015**, *61* (10), 3249–3269.
- (96) Valsecchi, M.; Galindo, A.; Jackson, G. Modelling the Thermodynamic Properties of the Mixture of Water and Polyethylene Glycol (PEG) with the SAFT- γ Mie Group-Contribution Approach. *Fluid Phase Equilib.* **2024**, *577*, No. 113952.
- (97) Wu, H. S.; Sandler, S. I. Use of ab Initio Quantum Mechanics Calculations in Group Contribution Methods. 1. Theory and the Basis for Group Identifications. *Ind. Eng. Chem. Res.* **1991**, *30* (5), 881–889.
- (98) Crespo, E. A.; Coutinho, J. A. P. A Statistical Associating Fluid Theory Perspective of the Modeling of Compounds Containing Ethylene Oxide Groups. *Ind. Eng. Chem. Res.* **2019**, *58* (9), 3562–3582.
- (99) Breil, M. P.; Kontogeorgis, G. M. Thermodynamics of Triethylene Glycol and Tetraethylene Glycol Containing Systems Described by the Cubic-Plus-Association Equation of State. *Ind. Eng. Chem. Res.* **2009**, *48* (11), 5472–5480.
- (100) Qvistgaard, D.; Kruger, F.; Liang, X.; Kontogeorgis, G. M.; von Solms, N. New Association Schemes for Tri-ethylene Glycol: Cubic-Plus-Association Parameterization and Uncertainty Analysis. *Fluid Phase Equilib.* **2022**, *551*, No. 113254.
- (101) Crespo, E. A.; Coutinho, J. A. P. Insights into the Limitations of Parameter Transferability in Heteronuclear SAFT-type Equations of State. *arXiv (Condensed Matter, Statistical Mechanics)* November 8, 2022, 2211.04606, version 1 (accessed January 10, 2023).
- (102) Li, J.; Chen, C.; Wang, J. Vapor-Liquid Equilibrium Data and their Correlation for Binary Systems Consisting of Ethanol, 2-Propanol, 1,2-Ethanediol and Methyl Benzoate. *Fluid Phase Equilib.* **2000**, *169* (1), 75–84.
- (103) Brinkley, R. L.; Gupta, R. B. Intra- and Intermolecular Hydrogen Bonding of 2-Methoxyethanol and 2-Butoxyethanol in n-Hexane. *Ind. Eng. Chem. Res.* **1998**, *37* (12), 4823–7.
- (104) Rowley, R. L.; Hoffman, G. L. Vapor-Liquid Equilibrium Measurements on Mixtures Important to Industrial Design: Triethylene Glycol + n-Hexane, Triethylene Glycol + Cyclohexane, and Furfural + Isoprene. *AICHE Symp. Ser.* **1990**, *279* (86), 6–19.
- (105) Oexmann, J.; Kather, A. Minimising the Regeneration Heat Duty of Post-Combustion CO₂ Capture by Wet Chemical Absorption: The Misguided Focus on Low Heat of Absorption Solvents. *Int. J. Greenh. Gas Control* **2010**, *4* (1), 36–43.
- (106) Cerdeiriña, C. A.; González-Salgado, D.; Romani, L.; Del Carmen Delgado, M.; Torres, L. A.; Costas, M. Towards an Understanding of the Heat Capacity of Liquids. A Simple Two-State Model for Molecular Association. *J. Chem. Phys.* **2004**, *120* (14), 6648–59.
- (107) Marshall, B. D.; Chapman, W. G. Resummed Thermodynamic Perturbation Theory for Bond Cooperativity in Associating Fluids. *J. Chem. Phys.* **2013**, *139* (21), No. 214106.
- (108) Jahn, D. A.; Akinkunmi, F. O.; Giovambattista, N. Effects of Temperature on the Properties of Glycerol: A Computer Simulation Study of Five Different Force Fields. *J. Phys. Chem. B* **2014**, *118* (38), 11284–94.